IMPROVING COOLING EFFICIENCY OF SERVERS BY REPLACING SMALLER CHASSIS ENCLOSED FANS WITH LARGER RACK-MOUNT FANS

by

BHARATH NAGENDRAN

Presented to the Faculty of the Graduate School of

The University of Texas at Arlington in Partial Fulfillment

of the Requirements

for the Degree of

MASTER OF SCIENCE IN MECHANICAL ENGINEERING

THE UNIVERSITY OF TEXAS AT ARLINGTON

December 2013

Copyright © by Bharath Nagendran 2013

All Rights Reserved

Acknowledgements

I would like to thank Dr. Dereje Agonafer for his continuous guidance and support over the last two years of my study and research at The University of Texas at Arlington.

I would like to thank Dr. Haji-Sheikh and Dr. Kent Lawrence for evaluating my work as committee members.

I thank Dr. Veerendra Mulay from Facebook Inc. for being part of my evaluating committee and for his technical guidance provided through my tenure at the University

I thank John Fernandes and Rick Eiland for being my technical mentors in accomplishing this work.

I thank my parents and uncles for encouraging me and funding my studies at the University.

I thank almighty god for providing me the strength and inspiration.

November 01, 2013

Abstract

Improving Cooling Efficiency Of Servers By Replacing Smaller Chassis Enclosed Fans With Larger Rack-Mount Fans

Bharath Nagendran, MS

The University of Texas at Arlington, 2013

Supervising Professor: Dereje Agonafer

As a common practice in the data center industry, chassis fans are used to direct air flow independent from neighboring servers. However, these fans are less efficient compared to larger rack level counterparts and also operate at higher sound levels. In this study, a novel approach is proposed whereby the smaller chassis enclosed fans are replaced with an array of larger fans, installed behind the stacked servers that share air flow.

As a baseline study for comparison of the current scenario, a CPU dominated 1.5U Open Compute server, with four 60mm fans installed within the server, is characterized experimentally for its flow impedance, air flow rate, effect on die temperature and power consumption for various compute utilization levels. Larger fans with a square frame size of 80mm are carefully selected and individually characterized for their air moving capacity and power consumption. CFD is used to simulate the system of stacked servers and larger fans to obtain its flow characteristics and operating points. The fan power consumption of the larger fans is determined experimentally at these operating points replicated in an air flow bench. Comparing with the base line experiments, this study predicts a significant decrease in fan power consumption, without conceding the flow rate and the static pressure requirements of the server.

Table of Contents

List of Illustrations

List of Tables

Chapter 1

Introduction

1.1 Data Center: Energy usage and Efficiency

Data Centers are computing facilities that contain large number of information technology equipment used to process, store and transmit data. This equipment is mounted in standardized cabinets / racks. The power densities are several hundred times than traditional office buildings and require specialized approaches.

Power consumed by data centers worldwide increased by about 56% from 2005 to 2010 instead of doubling (as it did from 2000 to 2005), while in the US it increased by about 36%, as reported by J. Koomey [1] in the New York Times in July 2011. The data reported by Koomey mentions that total electricity use by data centers in 2010 is about 1.3% of all electricity use for the world, and 2% of all electricity use for the US.

Also, such huge amount of power consumption is not fully utilized for computing purpose alone. Power Usage Effectiveness (PUE) is a measure of ratio of the total energy to the energy consumed by IT equipment. In a survey conducted by Uptime Institute [2] in 2012, the global average PUE of data centers is between 1.8 and 1.89. This means, almost an equal amount of energy is spent in non-IT power like cooling, power transmission losses.

The electrical power consumed by the IT equipment is entirely converted to heat and it must be rejected to the outside environment and simultaneously the IT equipment is to be operated in a cooler atmosphere in the same room. Therefore, the conditioned cold air and the rejected hot air must be directed effectively and efficiently in a data center. The increasing power densities of the IT equipment make it one of the biggest challenges in running data centers.

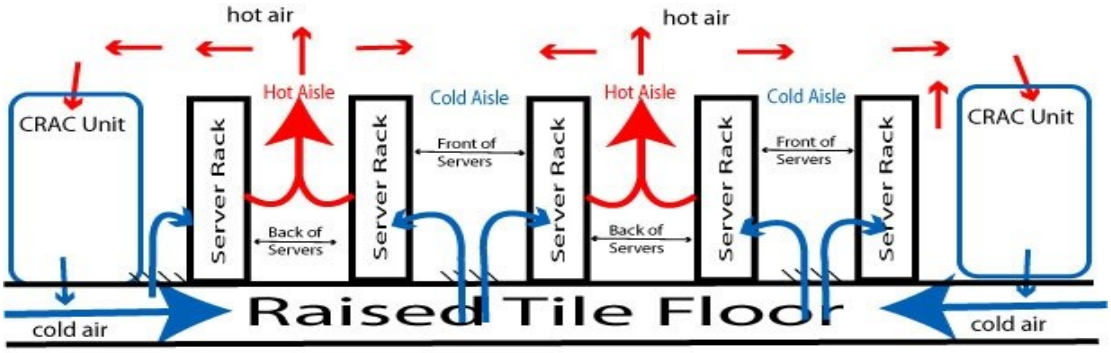

Figure 1.1: Typical thermal layout of a data center [3]

1.2 Multi-Level Thermal Management of Data Centers

With increase in power densities and need for efficient thermal management of data centers, a holistic consideration of rejection of heat from transistors and interconnects at nanometers, to the room facility with size of hundreds of meters is essential. The different levels of thermal management which needs attention are chip level, server level, rack level and room level.

Chip level thermal management includes heat dissipation techniques from the chip directly, like design of effective heat sink, use of thermal interface materials and heat spreader. Server level solutions considers heat rejection from the printed circuit board like fan installation and ducting air-delivery pathway to the heat sinks. Rack level design optimization enhances airflow within cabinets, placement of servers and liquid cooled cabinets. Room level cooling is achieved through computer room air-conditioning (CRAC) units that deliver cold air through perforated tiles.

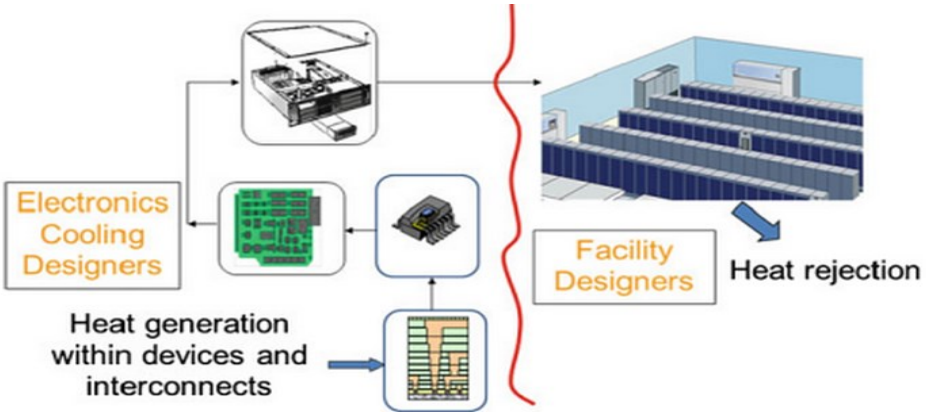

Figure 1.2: Multi-Scale nature of thermal management in data centers [4]

1.3 Motivation of the work

S. Balmer [5] mentioned in *Worldwide Partner Conference* 2013 hosted by Microsoft Corporation that the company has over a hundred thousand servers in their data center infrastructure and other IT majors also have almost similar numbers. With such huge number of servers, even a small saving in power consumption would scale up to be beneficial to these companies.

The power consumed by chassis fans and inefficiency of power supply units are parasitic loads attached to the server and thus needs to be maintained as minimal as possible. The objective of this work is to reduce cooling power of server by replacing smaller chassis fans by larger fans.

Figure 1.3, shows a graph from AMCA plotted between peak total efficiency and impeller diameter for homologous fans. It can be seen that below a threshold limit, the peak total efficiency is less for smaller diameter fans and it is therefore not desirable to select fan in this region. Also larger diameter fan shall affect the cooling redundancy of IT equipment.

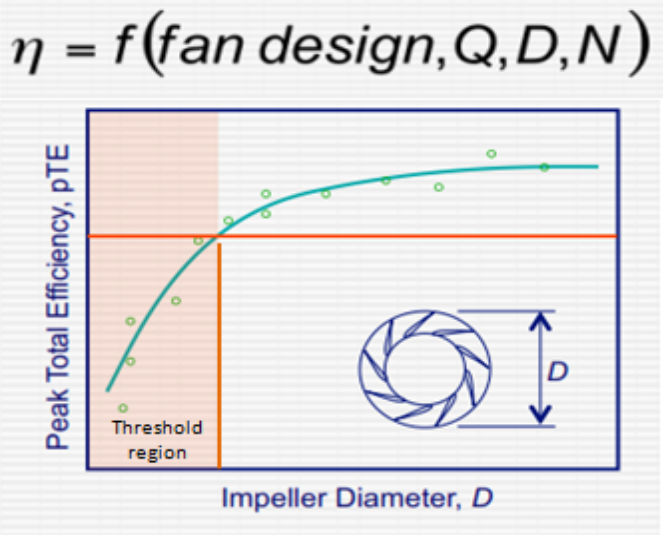

Figure 1.3: Peak total efficiency and impeller diameter [6]

This work has experimental and computational components to establish the case that the selected larger fan saves cooling power by its higher efficiency. Also fan failure study is performed to study the redundancy aspect of selecting the fans.

Chapter 2

Fans And Flow Characteristics In Electronic Equipment

2.1 Fans in electronic cooling industry

Fans are air moving devices which deliver air at a definite flow rate and static pressure. The commonly used fans in electronic equipment are axial fans which deliver air parallel to the rotor axis and centrifugal blowers which deliver air perpendicular to the rotor axis. Axial fans are installed in servers generally have high flow rate capacity and work against low static pressure. Blowers are installed in electronic equipment like laptops and it works against higher static pressure and low flow rate capacity.

2.2 Air moving capacity of a fan

Air moving capacity of a fan is specified by two parameters which are flow rate and static pressure. If a fan is operated in a condition such that there is no obstruction for air flow through the upstream and downstream and both are maintained at atmospheric pressure, then this condition is referred as free flow condition. The flow rate of the air blown by the fan in this condition is reffered as the maximum flow rate capacity of the fan. When the downstream side of the same fan is sealed to a closed chamber and the upstream is still maintained open to atmosphere, the fan pressurizes the chamber by forcing the atmospheric air into the chamber. As the pressure increases in the chamber, the flow rate into the chamber reduces. The point beyond which fan is not able to increase the pressure any further is reffered as the maximum static pressure capacity of the fan. At this point there will not be flow between the atmosphere and the chamber through the fan, because the entire energy (neglecting the ineffciencies) is utilized only to maintain the pressure in the chamber and this point is called stall point.

2.3 Reading a fan performance curve

Fan performance curve, also referred as fan curve, is a graphical representation of the air moving capacity of a fan. The graph is plotted against flow rate (x - axis) and static pressure (y - axis). Referring to figure2.1, point 1(x-intercept) represents free flow condition, where flow rate is maximum and static pressure is zero. Point 2 (y – intercept) represents stall condition where static pressure is maximum and flow rate is zero.

An air flow bench which can measure the flow rate and static pressure simulateously is used to determine the fan performance. For stall condition, all the nozzles are closed and the static pressure is measured. For free flow condition, the maximum flow rate is measured by making static pressure as zero by adjusting blower frequency.

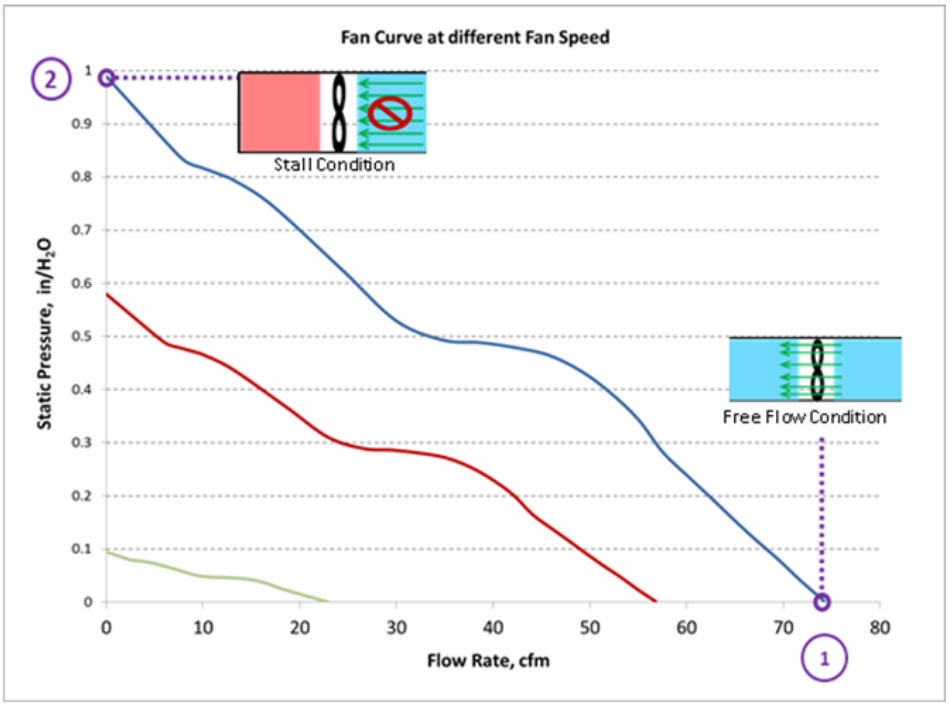

Figure 2.1: Fan Performance Curve – (source: experimental values)

2.4 Fan Laws

There are three fan laws used to interpolate flow rate, static pressure and air power from known values for different fan speed and diameter.

Fan Law 1:	$\frac{Q1}{Q2} = \left(\frac{N1}{N2}\right)\left(\frac{D1}{D2}\right)^3$
Fan Law 2:	$\frac{\Delta P1}{\Delta P2} = \left(\frac{N1}{N2}\right)^2\left(\frac{D1}{D2}\right)^2$
Fan Law 3:	$\frac{P1}{P2} = \left(\frac{N1}{N2}\right)^3\left(\frac{D1}{D2}\right)^5$

Figure 2.2: The three fan laws

where Q is Flow Rate, ∆P is Pressure Drop, P is Air Power, N is fan speed in RPM, D is Fan Impeller Diameter. These fan laws are derived from various ways of reasoning and mathematical approach like dimensional analysis. As derived by Jorgenson and Bohanon [7], setting compressibility coefficient ratio equal to unity, the laws for incompressible version can be obtained. Following is a simple way of reasoning to understand the origin of these laws.

Flow rate coefficient: $Q \propto A.V$ [Area(A) $\propto D^2$ and Velocity(V) $\propto DN$]

$\Rightarrow Q \propto (D^2).(DN)$

$\Rightarrow Q \propto (D^3N)$

Pressure drop coefficient: $\Delta P \propto V^2$ [From Bernoulli's Principle]

$\Rightarrow \Delta P \propto (DN)^2$

Power coefficient: P = Static Pressure x Flow Rate

$\Rightarrow P \propto \Delta P \,.\, Q$

$\Rightarrow P \propto (DN)^2.(D^3N)$ [From above two laws]

$\Rightarrow P \propto D^5.N^3$

Figure 2.3: Simple reasoning for fan law

In figure 2.1, the two fan curves between maximum fan speed and the origin, (red and green curve) can be obtained from fan laws for the corresponding fan speeds. It can be noted that the curve closer to origin is more flat than the farthest one, which is because the flow rate varies directly to fan speed ratio but the pressure varies to the square of fan speed ratio

2.5 Fans working in series and parallel combination

If “n” number of fans are in series, static pressure will increase “n” times for a given flow rate. If “n” numbers of fans work in parallel, flow rate will increase “n” times for a given static pressure. Series fans are used for system with higher flow resistance, while parallel fans are used for system with lower flow resistance.

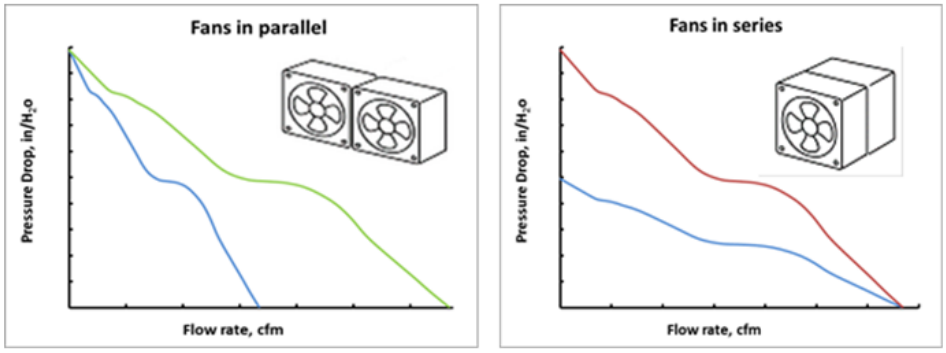

Figure 2.4: Fans in Parallel and Series combination

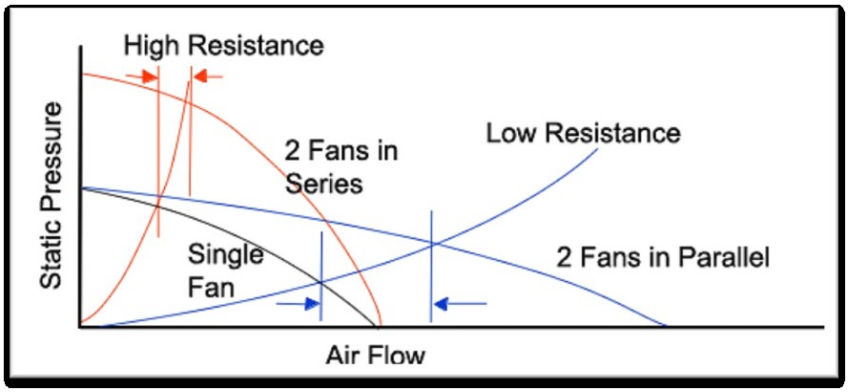

Figure 2.5: Use of fans in combination for high and low resistance system [8]

2.6 System Resistance

ASHRAE recommends an environment for safe operation of IT equipment by means of four parameters and has established standards for the same. These parameters are Inlet Air Temperature, Inlet Relative Humidity, Inlet Particulate Contamination and Inlet Gaseous Contamination. Even though these parameters may ensure the environment to be safe, the flow rate through each server is highly significant in safe operation of IT equipment and is not well defined by any standards until 2013. The flow rate through IT equipment, such as a server, depends on its flow resistance characteristics.

An IT equipment is fully populated with electronic components like capacitors, voltage regulators and heat rejection devices like heat sink. As air is passed through these components which obstruct the flow, energy loss is incurred is measured in terms of pressure drop and decrease in flow rate. Graphical representation of the flow resistance of the system is referred as system resistance curve.

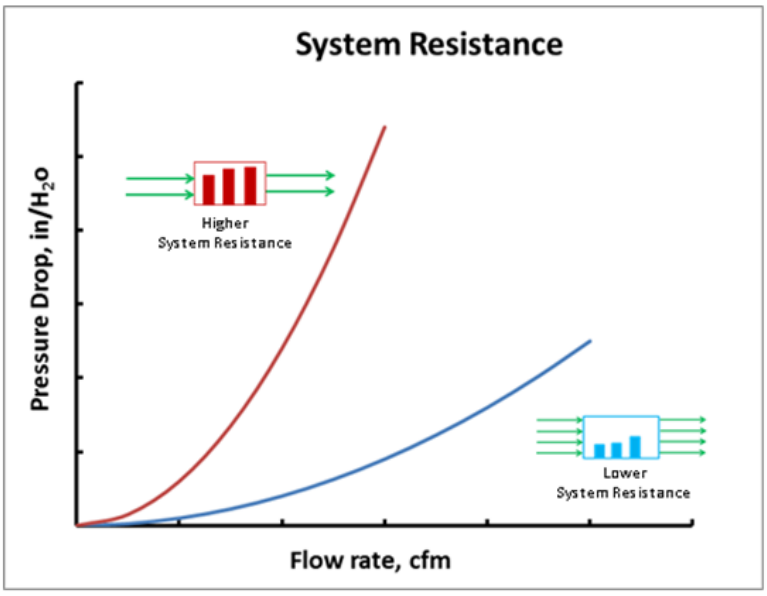

Figure 2.6: Depiction of high and low flow resistant system

For illustrative purposes, if a resistance curve coincides with horizontal axis (figure 2.4), such a system would offer no resistance to flow. On the other hand, if a resistance curve coincides with vertical axis it would represent a system which is fully blocked and there is no flow possible. As system resistance curve tends to move towards the vertical axis, it represents higher resistive flow as depicted in the figure. The system resistance is a flow property of the system only and the definition of a system shall not include the fan, while measuring the resistance curve.

When identical servers are stacked up, the system offers same resistance for the corresponding velocity. But as the flow area increases, due to stacking up of servers, the flow rate should also be increased to obtain the corresponding velocity and pressure drop.

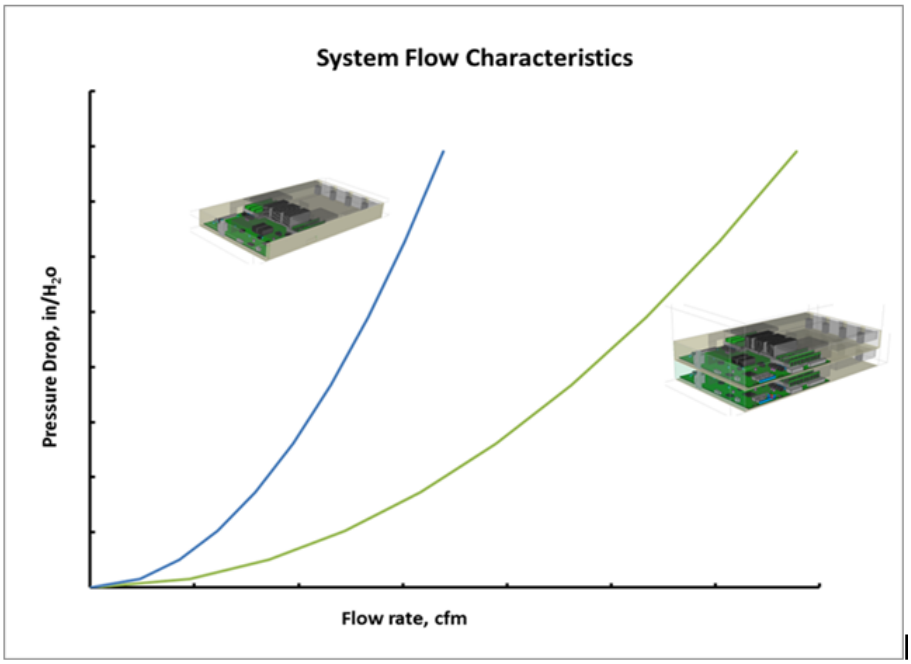

Figure 2.7: System resistance curve when identical servers are stacked up

2.7 Operating Point

The point where the system resistance curve meets the fan curve is called as the operating point. It is important to note that, the system may not refer to just a single server and the fan curve may not refer the performance of single fan. Effect of stacking up of servers and combination of fans shall be considered, if so.

As mentioned in previous section, the system resistance curve is a property of the system which graphically depicts the flow requirement. Similarly, fan curve is the stand-alone property of a fan which graphically depicts the air supply capacity of a fan at various static pressures. Therefore the point where both these curves meet represents the rate of air flow consumed by the system at the corresponding operating pressure (as in where supply and demand meets, is the actual consumption).

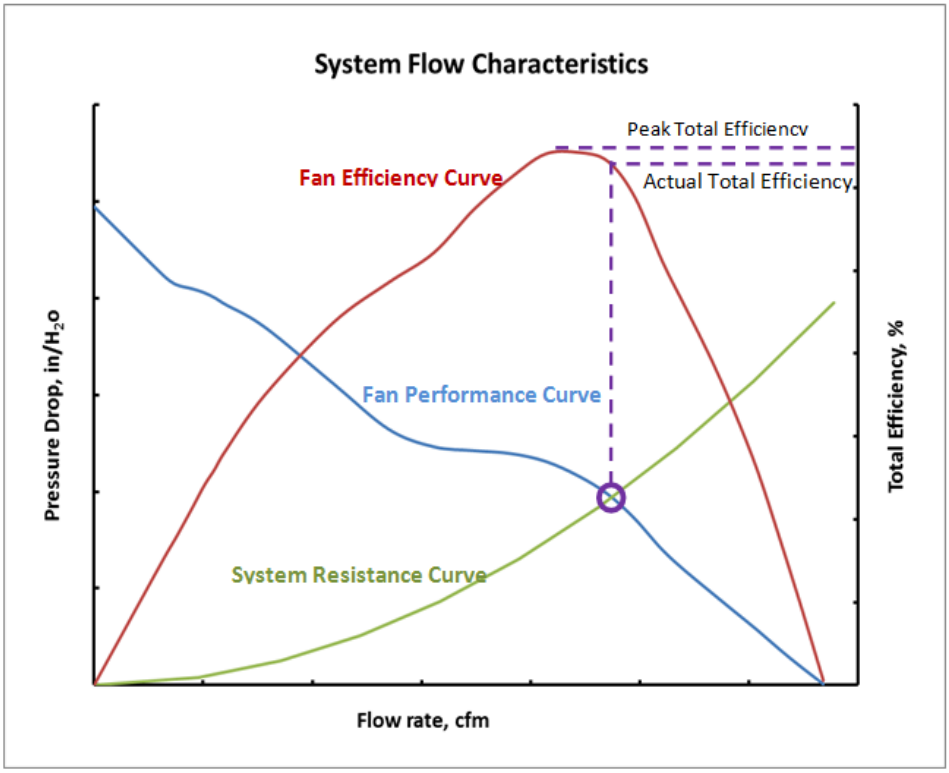

Figure 2.8: Operating Point of a System

Fans shall be selected in such a way that the operating point is closest to the peak total efficiency of the fan. Usually (PTE) peak total efficiency lies in the right half of the fan curve as shown in figure 2.6. The maximum required flow rate of system is based on the heat to be removed which can be found by CFD simulations.

Chapter 3

Experimental Characterization Of The Current System

3.1 Server under consideration

The system under study is an Intel based Open Compute 1.5U server [9], as shown in figure-3.1. The server has two CPUs (Intel Xenon 5650) with each one having a Thermal Design Power of 95W [10]. The two CPUs contribute major part of the thermal load and therefore, this server is referred as a CPU dominated server. Two heat sinks are mounted on each CPU to enhance heat transfer and thus contribute primarily to the flow obstruction. There are DIMM slots for mounting memory sticks, along the direction of the flow. A ducky is provided at the top of the server which channelizes the flow through major heat generating components.

There are four fans installed at the rear end of the chassis to compensate for the pressure drop and maintain the required flow rate through the servers. Each fan has dimension of 60 x 60 x 25.4 [11], facilitated with a Pulse Width Modulation control and a hall sensor to detect fan speed on real time basis. There is an on-board fan control algorithm which controls the fan speed based on the feedback from the hall sensor output. The fan control algorithm has a designated target die temperature, based on which PWM signal increases the fan speed to draw additional air to cool the heat sinks.

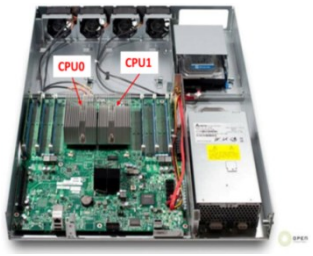

Figure 3.1: Intel based open compute server [9]

3.2 Current Scenario and modification

Four Sanace - 109R0612P4J06 fans are used in each server and thus for four stacked servers, there are 16 number of 60mm fans as shown in figure 3.2. It is to be noted that the chassis fans are completely enclosed inside the server which makes the flow inside each server independent from neighboring servers.

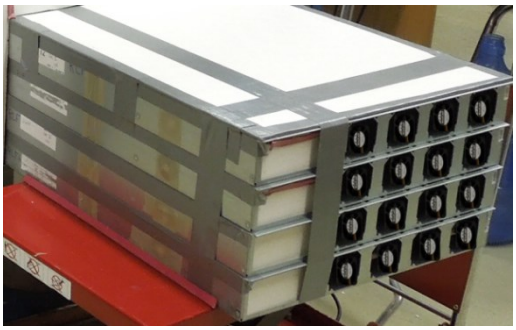

Figure 3.2: Four servers stacked up with fans enclosed inside

As mentioned in motivation (Section 1.3), this work aims at reducing the cooling power of the server by using larger fans which are more efficient than the smaller chassis fans enclosed in the chassis. The modification in this study is to replace the existing 60mm fans with larger 80mm fans. Four servers are stacked up and 9 fans of size 80mm are mounted behind the serves. The reasoning for this configuration is due to considerations in fan selection, which is detailed in the next chapter. As the 80mm fans cannot be enclosed inside 1.5U server, these fans are mounted rear to the servers as shown in figure 3.3.

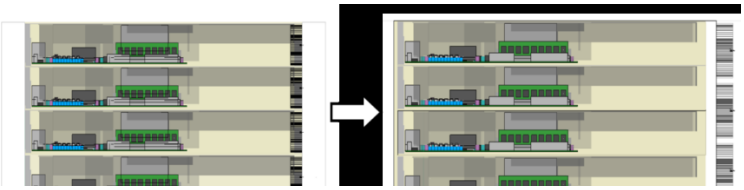

Figure 3.3: Modification of replacing 16 – 60mm fans to 9 – 80mm fans

3.3 Simplifying Assumptions

First simplifying assumption is to focus only on the motherboard section of the server, without the power supply unit (PSU) side. The PSU and hard disk is mounted separately in a channel, which is physically separated from the motherboard section of the server. Hence, the flow through PSU side does not affect the flow through motherboard section. Moreover, PSU has a separate fan which is controlled based on the inlet air temperature, unlike the fans in the motherboard section which are controlled based on CPU die temperature. Also, in general terms, the next generation servers have PSU located completely outside the chassis. With these considerations, this simplification is realistic.

Figure 3.4: Region under consideration [9]

Servers are stacked up with a view to mimic their operation in data centers. The computing load upon the servers is highly unpredictable and varies among different data centers. To consider the possible variations of utilization across the servers is beyond the scope of this work and therefore a simplification based on the following reasoning is considered.

Typically, at lower U_{CPU}%, the server power consumption rises steeply and tends to flatten at higher U_{CPU}% as shown in figure 3.5. Data centers operate at the flatter region of the curve to be cost effective. This study takes advantage of this condition and the CPU utilization levels (U_{CPU}) across the stacked servers is assumed to be uniform as illustrated in figure 3.6.

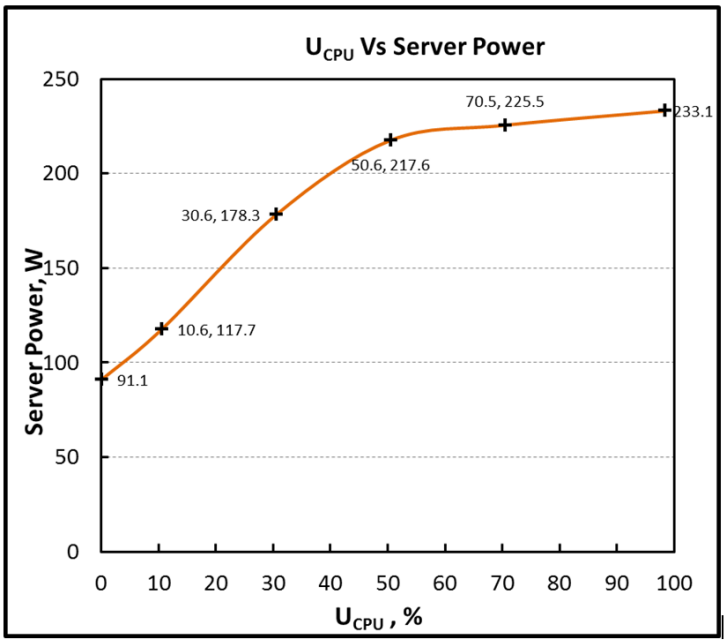

Figure 3.5: Plot based on experimental results for Server Consumption vs. U_{CPU}%

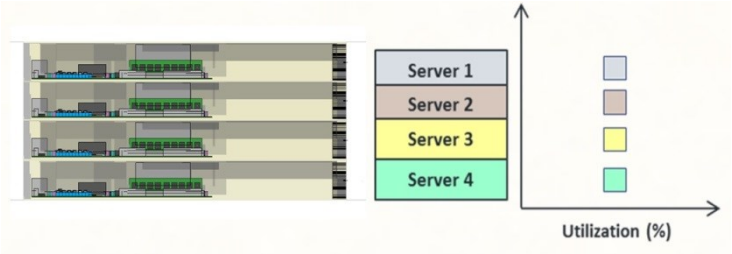

Figure 3.6: Uniform utilization across the stacked servers

3.6 Flow Characterization of the Base Line

Beginning from this section through the end of this chapter, results from experimental analysis of the base line scenario is presented. A single Open Compute Server with existing 60mm fans is referred to as the base line case, in order to compare these results with the proposed change. In this section in particular, the server is studied for its flow characteristics at constant ambient temperature of 24°C. Experiments to obtain data for system resistance curve, flow rate of the Server and individual fan curve are performed 3 times to ensure the repeatability.

3.6.1 System Resistance Curve

As discussed in section 2.6, system resistance curve graphically quantifies the flow resistance offered by a system against air flow. System resistance curve of a single server is obtained experimentally using air flow bench, with nozzle facing downstream as shown in figure 3.7.

The experimental results system resistance curve should comply with Bernoulli's Principle that the pressure drop shall be proportional to square of flow rate. Selection of nozzle should be appropriate to the corresponding flow rate; otherwise there will be significant deviation from the polynomial curve and the experimental data, at lower flow rates. The experimental result for system resistance curve of a single server is provided in table 3.1 and figure 3.8.

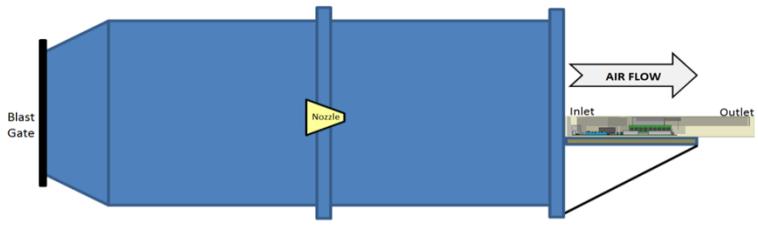

Figure 3.7: Schematic diagram of the experimental setup to find system resistance

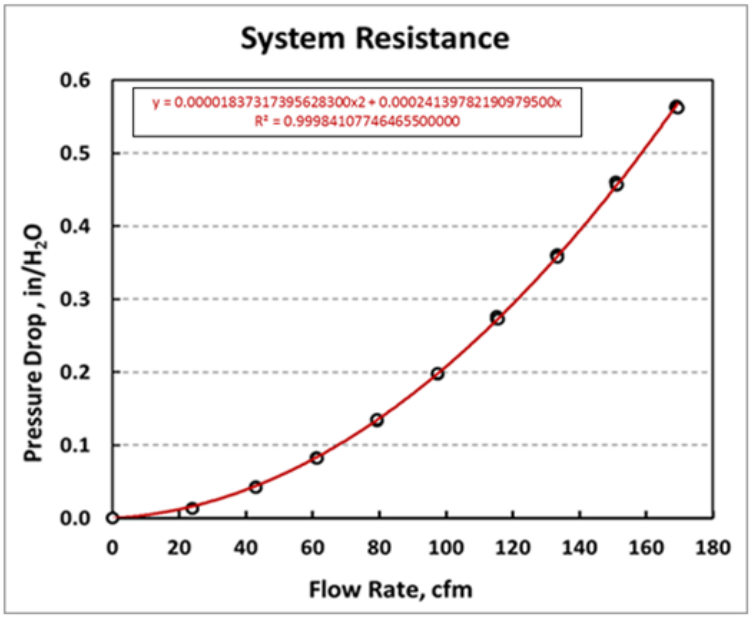

Figure 3.8: System Resistance curve for base line study

Table 3.1: Pressure drop values for various flow rates for the base line study

Experimental Result – System resistance	
Flow rate	**Static Pressure**
cfm	in/H_2O
0.0	0.000
24.0	0.013
42.9	0.043
61.3	0.083
79.3	0.136
97.3	0.198
115.1	0.273
133.4	0.358
151.0	0.456
169.1	0.565

3.6.2 Flow rate through the server

Flow rate of the server is obtained for various fan speed which is controlled by adjusting the PWM signal. As there are 4 fans in a server, fan speed is measured for one fan and plotted against total flow rate, as shown in figure 3.9. The duty cycle vs. flow rate is also plotted as this relationship would be helpful to have a common input parameter for all 4 fans. The maximum flow rate through the server is obtained at the 100% of the fan speed, which is 107cfm as in table 3.2.

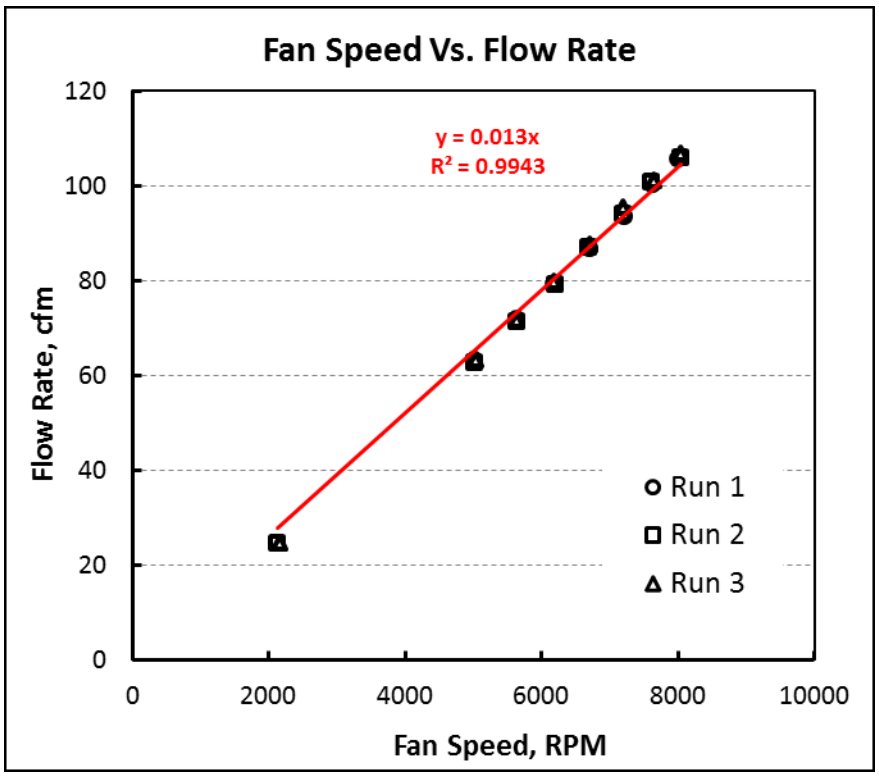

Figure 3.9: Fan Speed vs. Flow Rate for the base line study

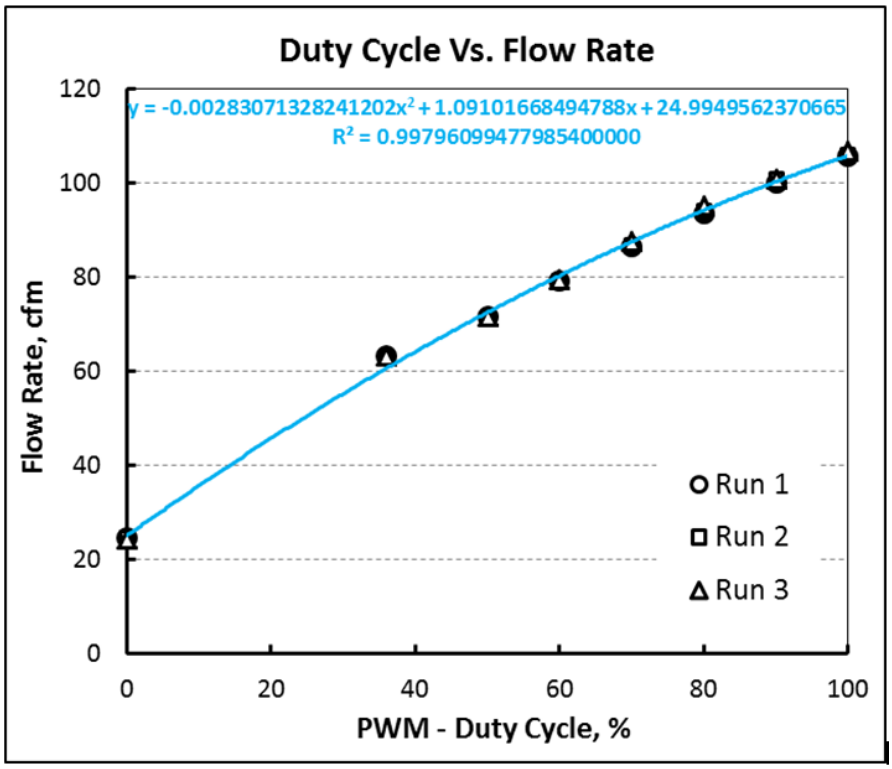

Figure 3.10: Duty Cycle vs. Flow Rate for the base line study

Table 3.2: Flow rate of the server for various fan speed and PWM duty cycle

Experimental Results – Flow rate		
PWM Duty Cycle	**Fan Speed**	**Flow Rate**
%	**rpm**	**cfm**
0	2161	24.40
36	5032	63.19
50	5642	71.49
60	6189	79.50
70	6710	87.49
80	7204	95.23
90	7648	100.86
100	8054	106.64

3.6.3 Fan Performance Characteristics (Sanace 109R0612P4J06)

In order to choose an alternative fan for the existing fan, performance of individual fan need to be obtained experimentally and verified with a refrence data. Manufacturer's data on the fan performance could be a valid reference for the experimental results. But the existing fans are tailored specifically for this application and references for the exact part number could not be obtained. However, the closest possible fan is identified as Sanace 109R0612P4J03 [12] and manufacturer's performance data is compared with the experimental results of the existing fan at 12V DC supply. Figure 3.11 shows that manufacturer's data has marginally higher capacity than existing fan, which can be accounted for leakage losses in air flow bench and accuracy of the pressure transducer.

Table 3.3: - Performance results for Sanace 109R0612P4J06

Experimental Results		**Manufacturer's data**	
Sanace 109R0612P4J06		Sanace 109R0612P4J03	
cfm	in/H_2O	cfm	in/H_2O
0.0	0.570	0.0	0.622
8.1	0.398	7.1	0.492
11.6	0.308	10.6	0.402
14.1	0.278	14.1	0.316
18.8	0.270	17.7	0.277
23.3	0.238	24.7	0.245
28.2	0.166	28.3	0.197
32.8	0.068	31.8	0.124
36.1	0.008	37.4	0.000

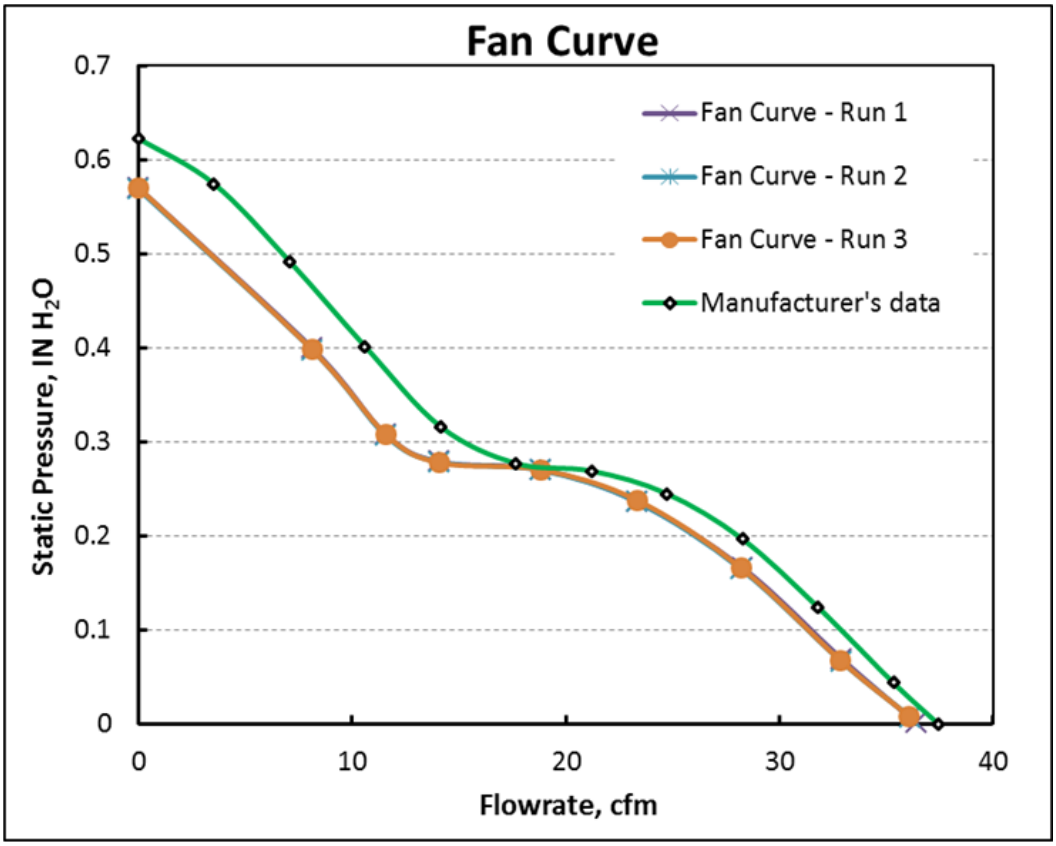

Figure 3.11: Fan Performance curve for Sanace 109R0612P4J06

3.7 Thermal and Power Characterization of the Base Line

While the flow characteristics depend on the layout and packaging of the electronic components in the server, the thermal and power characteristics depend on the performance of these electronic components. For the base line study, as the flow is independent from neighboring servers, thermal and power characteristics of a single server represents the behavior of other servers, which may be stacked.

3.7.1 Externally Controlled Fan Test

Series of experiments are conducted to study the effect of die temperature and server power by varying the fan speed externally. Fan speed is controlled by adjusting

the PWM duty cycle % using a function generator. Five different duty cycle % are considered, which are Idle (Ground), 35%, 60%, 80% and 100%. Equation in figure 3.10 (DC% vs. Flow rate) is correlated with test results in table 3.4 obtain relation between flow rate and fan power.

Lookbusy, a synthetic load generator is used load the CPU to various compute utilization levels. All the experiments are maintained at 24˚C and measurement is taken at approximately at 1 inch ahead of the server inlet using USB temperature data logger. Figure 3.12 shows the test cycle and duration of the load points.

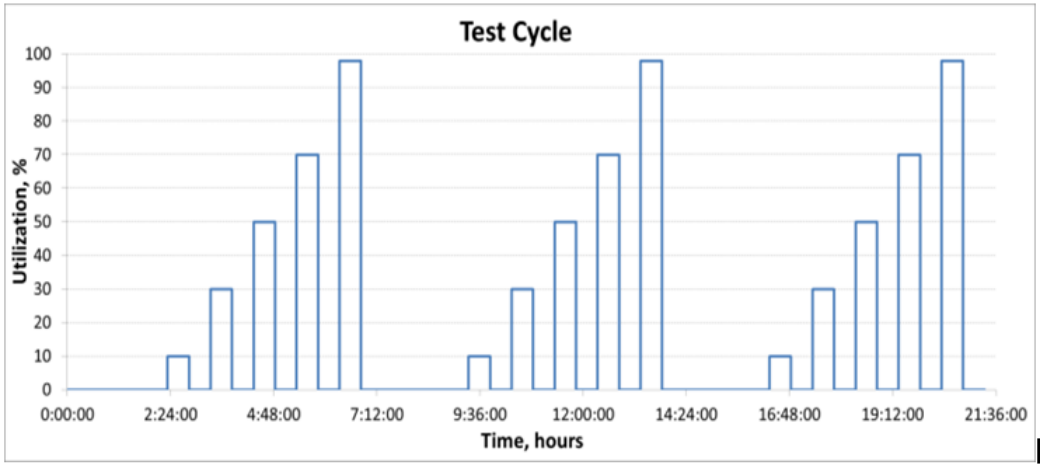

Figure 3.12: Test Cycle for various load points – Thermal and Power Characterization

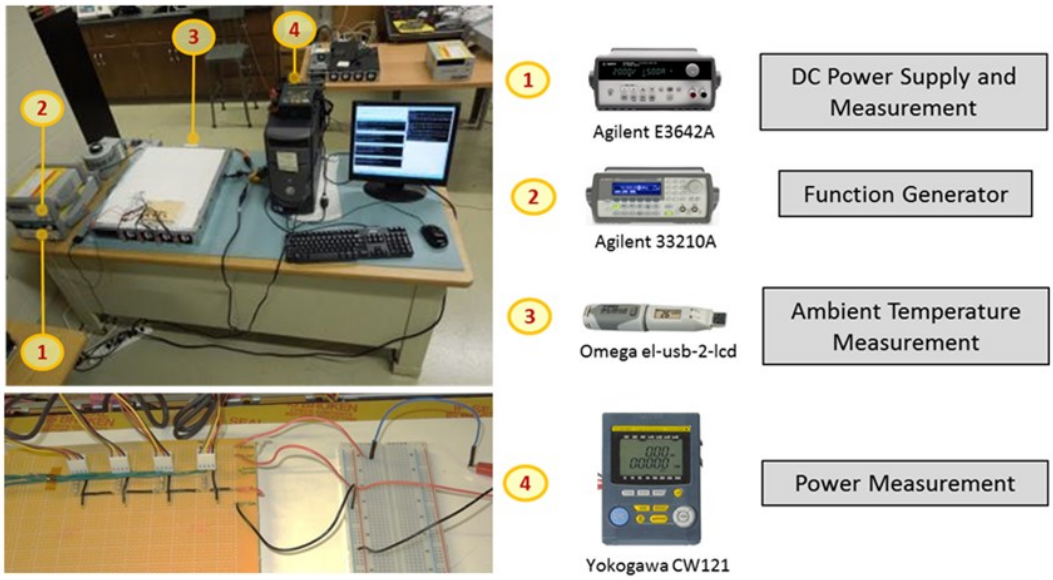

Figure 3.13: Experimental test set up – Thermal and Power Characterization

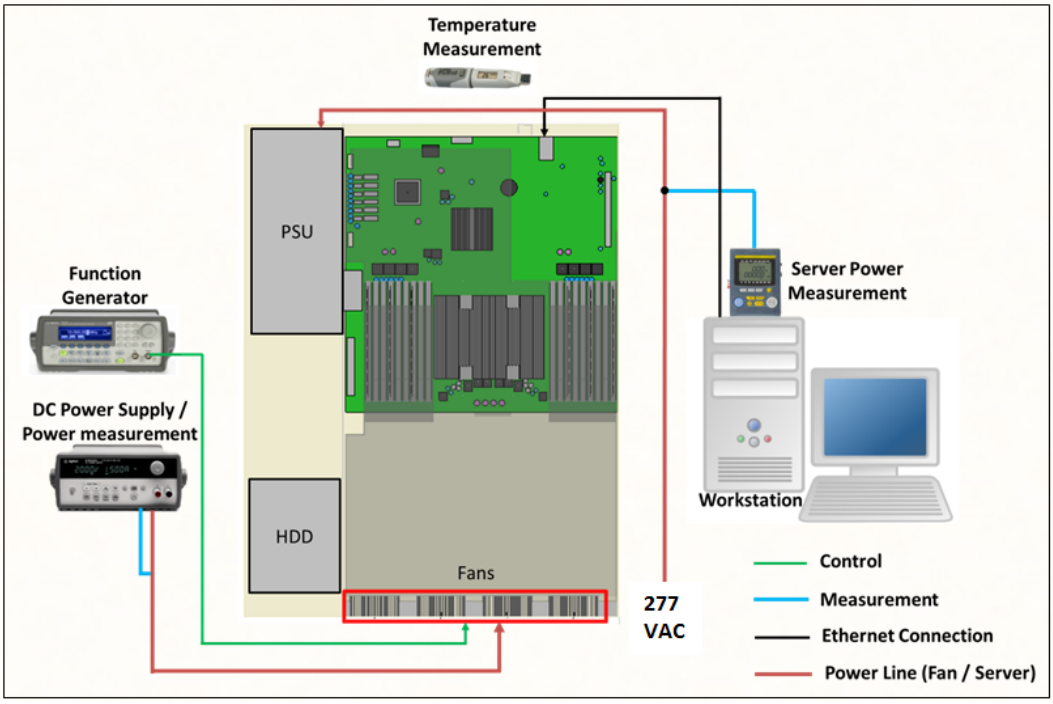

Figure 3.14: Schematic Diagram of the test set up – Power Characterization

Table 3.4: Test Results for Thermal and Power Characteristics – Externally Controlled Fans

Target Utilization	PWM	Ambient Temp	Actual Utilization	Memory	CPU 0 Die Temp	Server Power	Fan Power	Flow Rate	Total Power
%	%	°C	%	%	°C	W	W	cfm	W
Idle	Idle	24.0	0.2	0.8	32.2	90.2	2.3	25.0	92.6
	35	24.0	0.1	1.0	26.4	89.1	7.6	59.7	96.8
	60	24.0	0.1	0.8	25.4	89.1	11.0	80.3	100.1
	80	24.2	0.1	0.8	25.1	89.2	15.4	94.2	104.6
	100	24.0	0.1	0.8	25.0	89.1	20.0	105.8	109.0
10%	Idle	24.0	10.7	5.0	41.8	117.3	2.3	25.0	119.6
	35	24.0	10.6	5.1	32.5	114.7	7.6	59.7	122.4
	60	24.2	10.6	4.9	31.6	114.9	11.0	80.3	125.9
	80	24.1	10.6	4.9	30.5	114.7	15.4	94.2	130.1
	100	24.0	10.6	4.9	30.2	114.7	20.0	105.8	134.7
30%	Idle	24.0	30.7	5.0	64.6	177.9	2.3	25.0	180.3
	35	24.0	30.6	5.1	44.9	171.1	7.6	59.7	178.7
	60	24.2	30.6	4.9	43.7	169.7	11.0	80.3	180.7
	80	24.1	30.6	4.9	43.0	170.7	15.4	94.2	186.1
	100	24.0	30.6	4.9	41.9	170.4	20.0	105.8	190.3
50%	Idle	24.2	50.6	5.0	78.3	219.5	2.3	25.0	221.8
	35	24.0	50.5	5.1	54.4	212.1	7.6	59.7	219.8
	60	24.0	50.5	4.9	52.5	211.0	11.0	80.3	222.0
	80	24.2	50.5	4.9	51.0	210.9	15.4	94.2	226.3
	100	24.0	50.5	4.9	50.0	211.2	20.0	105.8	231.2
70%	Idle	24.2	70.6	5.0	82.1	229.9	2.3	25.0	232.3
	35	24.0	70.5	5.1	55.6	217.5	7.6	59.7	225.1
	60	24.1	70.5	4.9	53.9	219.1	11.0	80.3	230.0
	80	24.0	70.5	4.9	52.3	218.9	15.4	94.2	234.3
	100	24.0	70.5	4.9	51.3	218.6	20.0	105.8	238.6
98%	Idle	24.2	98.5	5.0	87.0	237.2	2.3	25.0	239.5
	35	24.0	98.5	5.2	57.8	224.1	7.6	59.7	231.8
	60	24.1	98.5	4.9	55.3	223.4	11.0	80.3	234.4
	80	24.0	98.5	4.9	53.8	223.1	15.4	94.2	238.4
	100	24.0	98.5	4.9	53.0	223.1	20.0	105.8	243.0

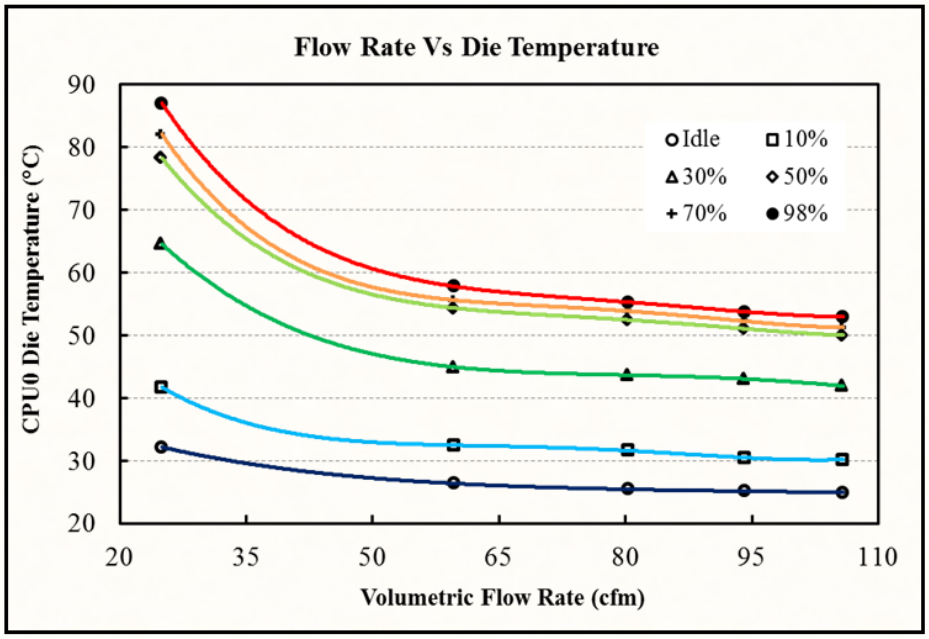

Figure 3.15: Plot representing Die Temperature vs. Flow Rate for Utilization Levels

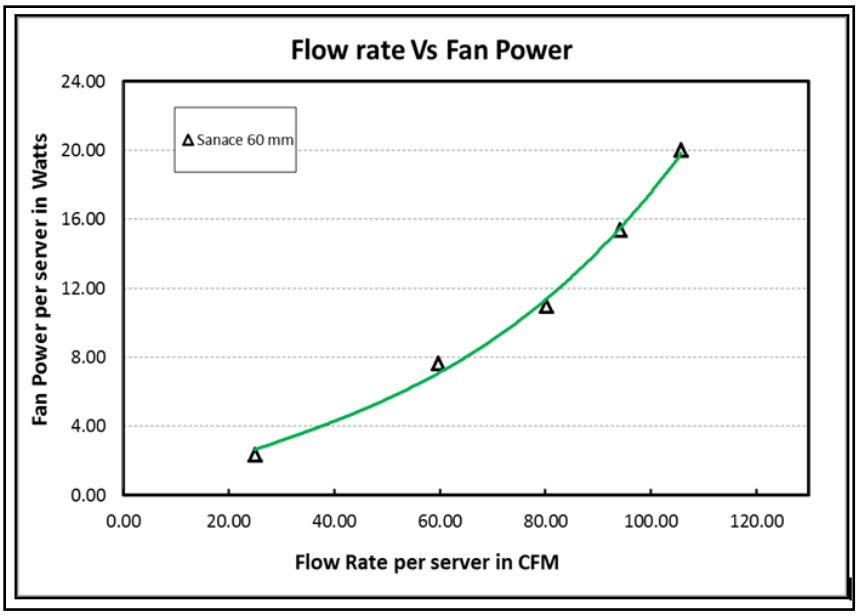

Figure 3.16: Plot representing Flow Rate vs. Fan Power for 60mm fans

From figure 3.15, it can be noted that, as the flow rate increases, the die temperature decreases, but there is a reduction in the rate at which temperature decreases as the heat transfer is jeopardized by the inlet ambient temperature. Also, for a given flow rate, the die temperature at higher utilization levels remains almost same. This is an important reason for the assumption uniform utilization mentioned in section 3.3 is realistic. It is important to recognize that this relation of die temperature and flow rate is independent of the fan being used. Therefore this relation will be used for similar scenario of larger fans to deduce some significant observations.

The flow rate vs. fan power is plotted in figure 3.16, where the maximum flow rate is 106 cfm with power consumption of 20W and the minimum flow rate is 25 cfm with a power consumption of 2.3 W.

3.7.2 Internally Controlled Fan Test

A similar test is conducted except for the fan speed which is controlled by the on-board fan control algorithm. The table showing the results and the plots are given below.

Table 3.5: Test Results for Thermal and Power Characteristics – Internally Controlled Fans

Target Utilization	Amb. Temp	%CPU	%MEM	CPU0 DT	Speed - Fan 1	Speed - Fan 2	Speed - Fan 3	Speed - Fan 4	Server Power	Fan Power	Total power
%	°C	%	%	°C	RPM	RPM	RPM	RPM	W	W	W
Idle	24	0.1	1.0	32.7	2037	2032	1980	2022	91.1	2.37	93.4
10%	24	10.6	5.1	39.5	2043	2032	1983	2025	117.7	2.37	120.1
30%	24	30.6	5.1	64.6	2061	2041	1991	2037	178.3	2.37	180.7
50%	24	50.6	5.1	71.7	2388	2384	2313	2368	217.6	2.80	220.4
70%	24	70.5	5.1	73.6	2520	2513	2439	2498	225.5	2.88	228.4
98%	24	98.5	5.1	73.8	2648	2641	2544	2608	233.1	3.07	236.1

For lower utilization levels the die temperature being less, fan speed is maintained at lower levels, in order to save fan power. As the die temperature increases due to increase in utilization, the fan speed is also correspondingly increased by the control feature in the motherboard. This increases the fan power consumption and thus tries to maintain the die temperature at programmed target die temperature, as shown in the figure 3.17.

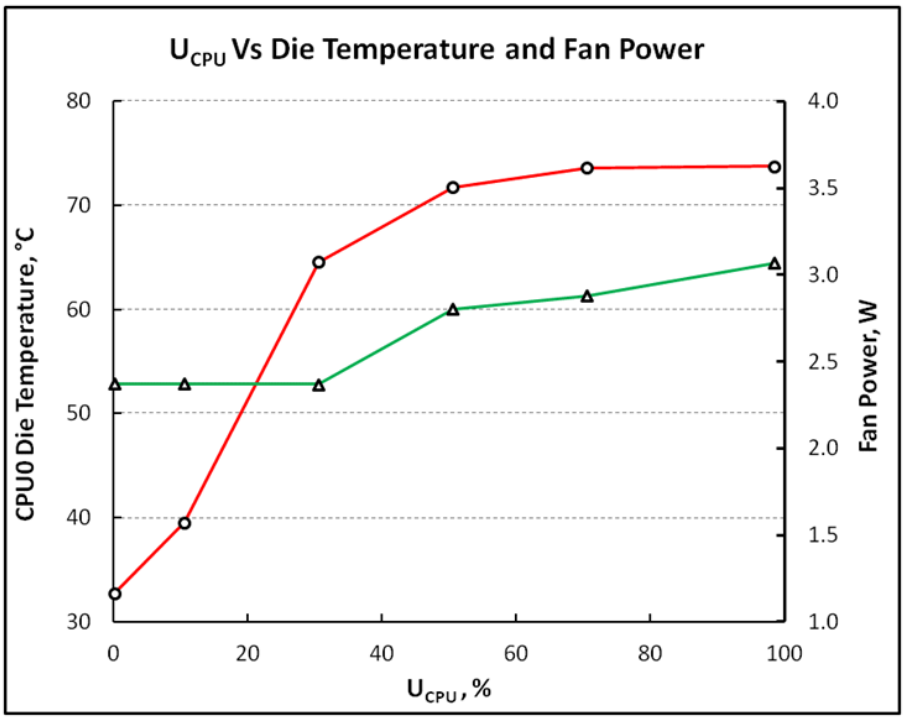

Figure 3.17: : Plot representing Die Temperature and Fan Power vs. Utilization

Chapter 4

Larger Efficient Fans

4.1 Fan Selection

Manufacturer's data of 60mm [12] fan is considered for fan selection purpose and interpolated for four fans using fan laws. The flow provided by four fans is the flow requirement of a single server. Flow selection criteria for a single server are, the flow rate at the free flow condition shall be greater than 150cfm (4 x 37.4cfm) and the maximum static pressure should be greater than 0.622 IN H2O. The maximum power consumption per server shall not exceed 20W.

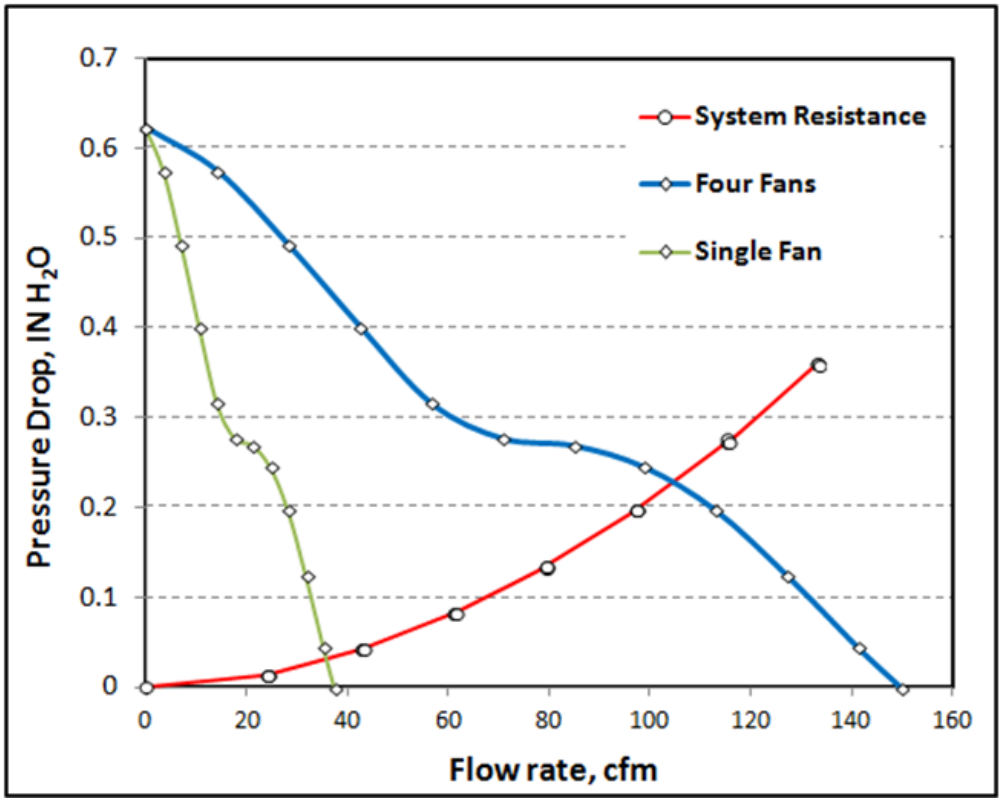

Figure 4.1: Flow selection criteria for a single server

Table 4.1: Fan considered from manufacturer's catalogue [13], [14], [15]

Number of fans across the width	1	2	3
Number of servers to be catered	5	2	4
Manufacturer	ebm-papst	Delta Fans	Sanyo Denki
Model No.	A1G280-AA79-11	QFR1212EHE	9GA0812P2H0011
Frame	Circular	Square	Square
Dimension	Ø 280 x 77.7	120 x 120 x 38	80 x 80 x 32
Max. Flow Rate (CFM) per Fan	1065	173.83	77.7
Number of fans	1	2	9
Total CFM	1065	347.66	699.3
Pressure Drop (in/H2O)	0.779	0.844	1.18
Power (W) per fan	90	12	7.08
dBA	63	59	54

There are three fans which can be considered based on the manufacturer's websites. Among the three options, Sanyo Denki (Sanace) 9GA0812P2H0011 is selected for further investigation. The other two options are eliminated considering redundancy, as each failed fan would wipe off huge amount of flow rate resulting hot air re-circulation between hot-aisle and cold-aisle containments and eventually increase the die temperature of the server to undesirable extent.

The number of servers to be stacked is selected as four, based on the form factor of the servers being stacked up and the fan performance characteristics. Even as 8 of the selected fan could satisfy the flow requirement for 4 servers, 9 of them are used in order to maintain uniform flow rate across the servers and to compensate during a fan failure scenario.

4.2 Flow Characterization of the Selected Fan

The fan curve is obtained at 12V using air flow bench testing and compared with the manufacturer's data which is at 13.8V. As the input voltage reduces the fan curve

tends towards origin. The maximum static pressure obtained at 12V is 0.989 IN-H2O and the flow rate is 74.2 cfm.

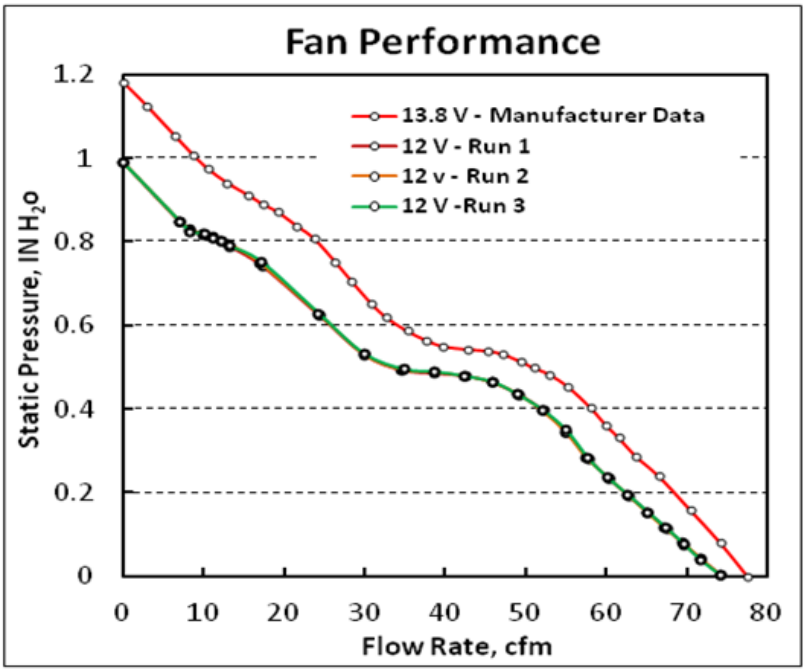

Figure 4.2: Fan Performance curve for Sanace 9GA0812P2H0011

Figure 4.3: Sanace 9GA0812P2H0011

[15]

4.3 Flow analysis using CFD

4.3.1 Flow modeling using 6SigmaET

Modeling of the system of servers and fans is carried out using commercially available software, 6SigmaET from *future facilities.* The experimental results for system resistance and fan performance are incorporated into the porous obstruction model. A porous obstruction is a simplified model of the actual system which replicates the flow in terms of the pressure drop across inlet and outlet, which is calculated based on the experimental results imparted into it. Using porous obstruction reduces the solving time drastically, but it cannot provide the flow visualization of the actual server, which is not required in this study.

The selected larger fans are placed behind the stacked servers and held equidistantly by the fan wall with a clearance between the rear end of the servers. Advanced grid generation is used near the fan wall and mesh sensitivity analysis is performed to ensure the numerical solution is independent of the grid size. In case of porous obstruction model, the solution becomes grid independent at highly course mesh as the model is mathematically inherent of the pressure drop characteristics.

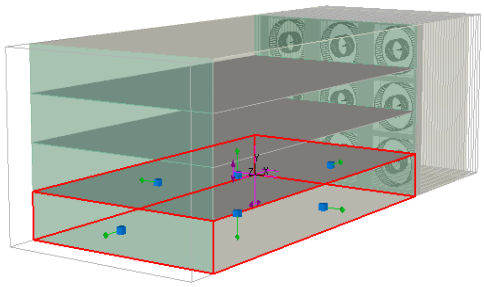

Figure 4.4: CFD Model - Porous Obstruction

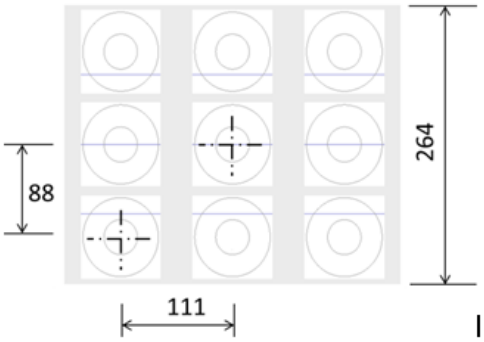

Figure 4.5: CFD Model - Fan spacing dimensions (mm)

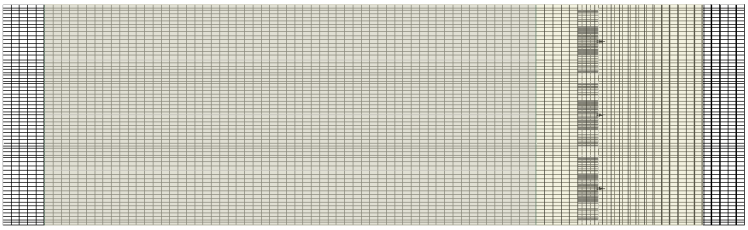

Figure 4.6: CFD Model - Meshing

◢ Grid	
Limit Maximum Cell Size	Yes
Max size in X	8 mm
Max size in Y	5 mm
Max size in Z	10 mm
Cell Count Target	100000
Minimum Gap Size	0.0005 m
Enable Heat Conduction Gridding	Yes
Use Advanced Grid Controls	Yes
Use Inflation	Yes
◢ Grid Summary	
Auto (Unlimited) Cell Count	645904
Grid Size	51 x 63 x 94 (302022 cells)
◢ Largest Cells	
Largest X	0.00775 @ 0.3175 m
Largest Y	0.005405 @ 0.060595 m
Largest Z	0.01 @ 0.2 m
◢ Smallest Cells	
Smallest X	0.0025 @ 0.0155 m
Smallest Y	0.0025 @ 0.1695 m
Smallest Z	0.001 @ 0.84 m
Maximum Aspect Ratio	7.75 (X/Z)
Maximum Expansion Ratio	10 @ Z = 0.84 m

Figure 4.7: CFD Model - Grid Size

4.3.2 Flow uniformity across the servers

CFD analysis is conducted to understand the flow uniformity across different server for various fan speeds. As these larger fans cannot be installed inside the server, these are mounted on a fan wall leaving a clearance distance between the fan wall and the rear end of the servers. Figure 4.5 shows the server arrangement and the numbering and table 4.2 shows variation of the flow rate across different servers for various fan speed.

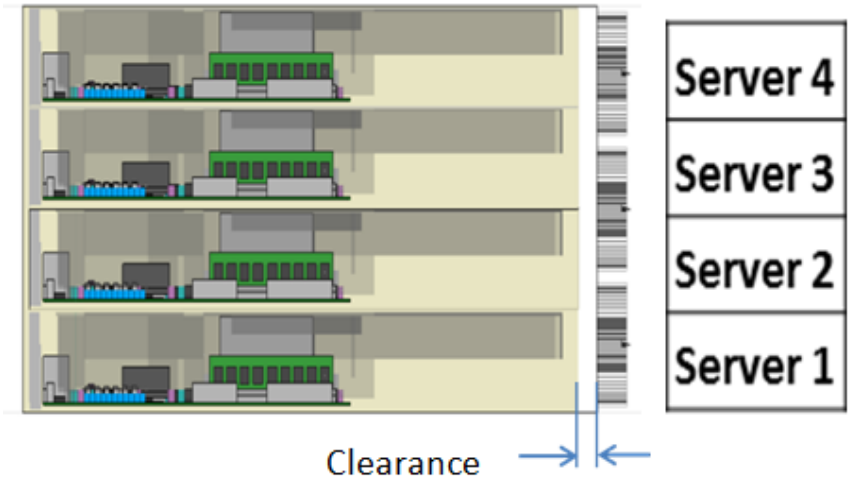

Figure 4.8: Server numbering

Table 4.2: Flow distribution across different servers for various fan speed

Clearance mm	Fan Speed RPM	Inlet Flow rate, cfm				Max. Difference cfm	Total flow rate cfm
		Server 1	Server 2	Server 3	Server 4		
0	8514	133.8	122.4	118	136.7	18.7	510.9
0	5904	92.13	84.14	81.15	94.1	12.95	351.52
0	2635	39.79	36.44	35.12	40.54	5.42	151.9

As the fan speed increases, the variation of the flow rate also increases. To capture the maximum flow rate variation, the maximum fan speed is simulated for various clearance values as in table 4.2.

Table 4.3: Flow distribution across different servers for various clearance distance

Clearance mm	Fan Speed RPM	Inlet Flow rate, cfm				Max. Difference cfm	Total flow rate cfm
		Server 1	Server 2	Server 3	Server 4		
0	8514	133.8	122.4	118	136.7	18.7	510.9
10	8514	128.7	126.7	126.4	129.5	3.1	511.3
20	8514	128.2	127.5	127.3	128.6	1.3	511.6
30	8514	128.1	127.6	127.6	128.3	0.7	511.6
40	8514	128	127.7	127.6	128.2	0.6	511.5
50	8514	127.9	127.6	127.6	128.1	0.5	511.2

The farther the fan wall is placed farther from the servers; the flow tends to be more uniform across the servers. But the fan wall needs to be well contained inside the rack which constraints the fan wall being away from the servers. With a clearance of 20mm between the server and the fan wall, the flow distribution is uniform enough and is placed well within the rack, as referred in figure 4.9 and table 4.3.

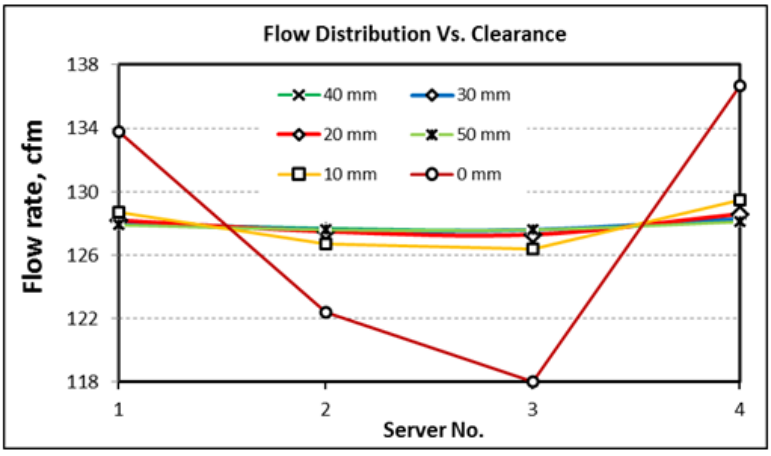

Figure 4.9: Plot for flow distribution vs. clearance

4.3.3 Determining operating points at different fan speed

As there are 9 fans which support 4 servers, the operating points of these fans are determined for various fan speeds using CFD and also validated using the fan laws. The following tables and figure illustrate these operating points and the comparison of the fan law calculation with CFD results.

Table 4.4: Determining Operating Points using CFD

PWM%	RPM @ free flow	CFM	STP
100	8514	56.9	0.290
90	8207	54.8	0.277
80	7722	51.5	0.246
70	7137	47.6	0.212
60	6517	43.4	0.178
50	5904	39.2	0.148
40	5318	35.2	0.121
30	4804	31.72	0.100
0	2635	17	0.033

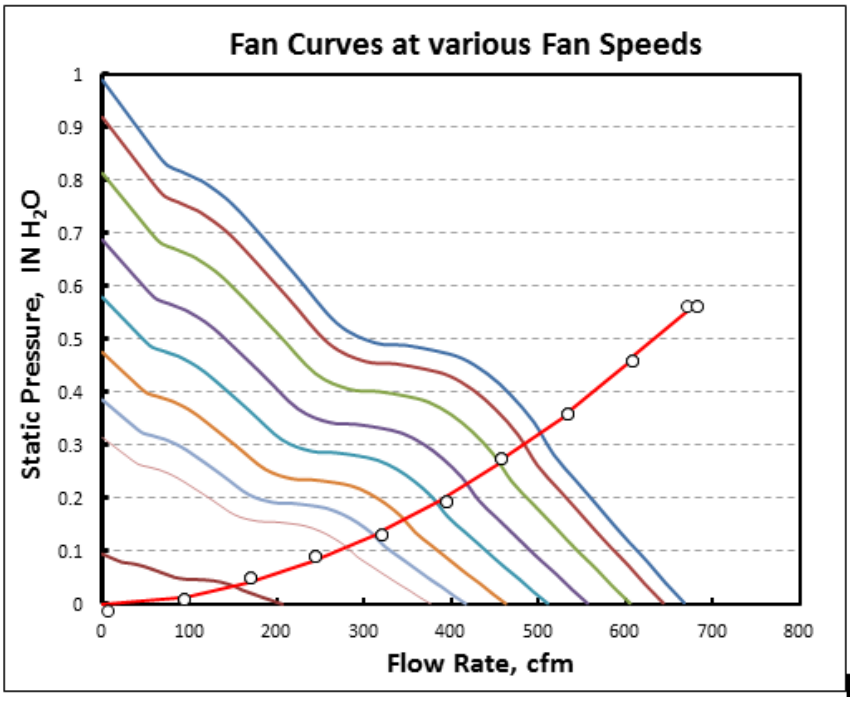

Figure 4.10: Determining Operating Points using Fan Laws

Table 4.5: Determining Operating Points using CFD

PWM%	RPM @ free flow	Flow rate cfm			Static Pressure in/H2O		
		CFD	Fan Law	Error %	CFD	Fan Law	Error %
100	8514	56.9	55.9	1.81	0.290	0.323	-10.22
90	8207	54.8	53.8	1.90	0.277	0.302	-8.28
80	7722	51.5	50.7	1.64	0.246	0.266	-7.41
70	7137	47.6	46.4	2.49	0.212	0.228	-7.02
60	6517	43.4	42.7	1.72	0.178	0.192	-7.24
50	5904	39.2	38.4	1.97	0.148	0.16	-7.50
40	5318	35.2	34.7	1.54	0.121	0.13	-6.85
30	4804	31.72	31.1	1.96	0.100	0.108	-7.41
0	2635	17	16.8	1.32	0.033	0.034	-2.94

4.4 Fan Power Measurement for larger fans

4.4.1 Experimental measurement of fan power at the operating points

As all the 9 fans in the fan array operates at the same operating point at a given speed, fan power of all the 9 fans can be estimated by a single fan. Thus the operating point at various speeds, as obtained from CFD results, is replicated in an air flow chamber and the corresponding fan power consumption is recorded.

The following tables provide the experimental data and the comparison between the target operating points and the operating point obtained from air flow chamber.

Table 4.6: Experimental results for fan power at the operating point

PWM	Run 1				Run 2				Run 3				Target Points	
	Flow Rate	STP	Fan Speed	Power	Flow Rate	STP	Fan Speed	Power	Flow Rate	STP	Fan Speed	Power	Flow Rate	STP
	CFM	IN H_2O	RPM	Watts	CFM	IN H_2O	RPM	Watts	CFM	IN H_2O	RPM	Watts	CFM	IN H_2O
100%	55.3	0.290	7932	7.1	55.9	0.291	7962	7.1	56.4	0.279	7953	7.1	56.9	0.29
90%	53.0	0.278	7630	6.6	53.4	0.275	7805	6.6	52.9	0.277	7649	6.6	54.8	0.277
80%	49.8	0.248	7166	5.6	50.4	0.246	7236	5.6	49.8	0.249	7204	5.5	51.5	0.2463
70%	45.9	0.215	6601	4.6	46.6	0.212	6684	4.7	46.1	0.215	6703	4.7	47.6	0.212
60%	41.9	0.183	6133	3.6	42.8	0.178	6193	3.7	42.3	0.176	6160	3.6	43.4	0.1781
50%	38.4	0.147	5611	2.9	38.3	0.148	5532	2.9	37.5	0.149	5515	2.9	39.2	0.148
40%	33.6	0.125	5078	2.3	34.0	0.121	5014	2.3	32.9	0.122	4978	2.3	35.2	0.1211
30%	29.9	0.098	4571	1.7	30.8	0.101	4607	1.8	29.6	0.100	4440	1.8	31.72	0.1
Idle	8.7	0.034	2450	0.6	8.7	0.034	2449	0.6	8.8	0.034	2452	0.6	17	0.033

Table 4.7: Difference between target point and the obtained point

	Static Pressure in in / H2O			Flow Rate in CFM		
	Experiment	Target	Difference	Experiment	Predicted	Difference
Run 3	0.279	0.290	-0.011	56.4	56.9	-0.5
	0.277	0.277	0.000	52.9	54.8	-1.9
	0.249	0.246	0.003	49.8	51.5	-1.7
	0.215	0.212	0.003	46.1	47.6	-1.5
	0.176	0.178	-0.002	42.3	43.4	-1.1
	0.149	0.148	0.001	37.5	39.2	-1.7
	0.122	0.121	0.001	32.9	35.2	-2.3
	0.100	0.100	0.000	29.6	31.72	-2.1
	0.034	0.033	0.001	8.8	17	-8.3

4.4.2 Flow Rate and Fan Power per Server

In order to compare the results with the base line study results (1 server with 4 - 60mm fans), the flow and power characteristics of 80mm fan is translated for a single server. Flow rate and fan power for a single server are estimated from the experimental data of a single fan by a multiplication factor of 9/4 (9 fans for four servers). The following table and the plot provide flow rate and fan power consumption calculated for a single server.

Table 4.8: Flow Rate and Fan Power per Server

PWM	Run 1		Run 2		Run 3	
	Power	Flow rate	Power	Flow rate	Power	Flow rate
	W	cfm	W	cfm	W	cfm
100%	15.93	124.31	15.93	125.87	15.93	126.81
90%	14.85	119.31	14.85	120.13	14.85	119.12
80%	12.69	112.01	12.69	113.40	12.42	112.01
70%	10.26	103.34	10.53	104.87	10.53	103.70
60%	8.10	94.34	8.37	96.26	8.10	95.15
50%	6.48	86.31	6.48	86.15	6.48	84.35
40%	5.13	75.60	5.13	76.48	5.13	73.98
30%	3.78	67.30	4.05	69.30	4.05	66.60
Idle	1.35	19.46	1.35	19.46	1.35	19.69

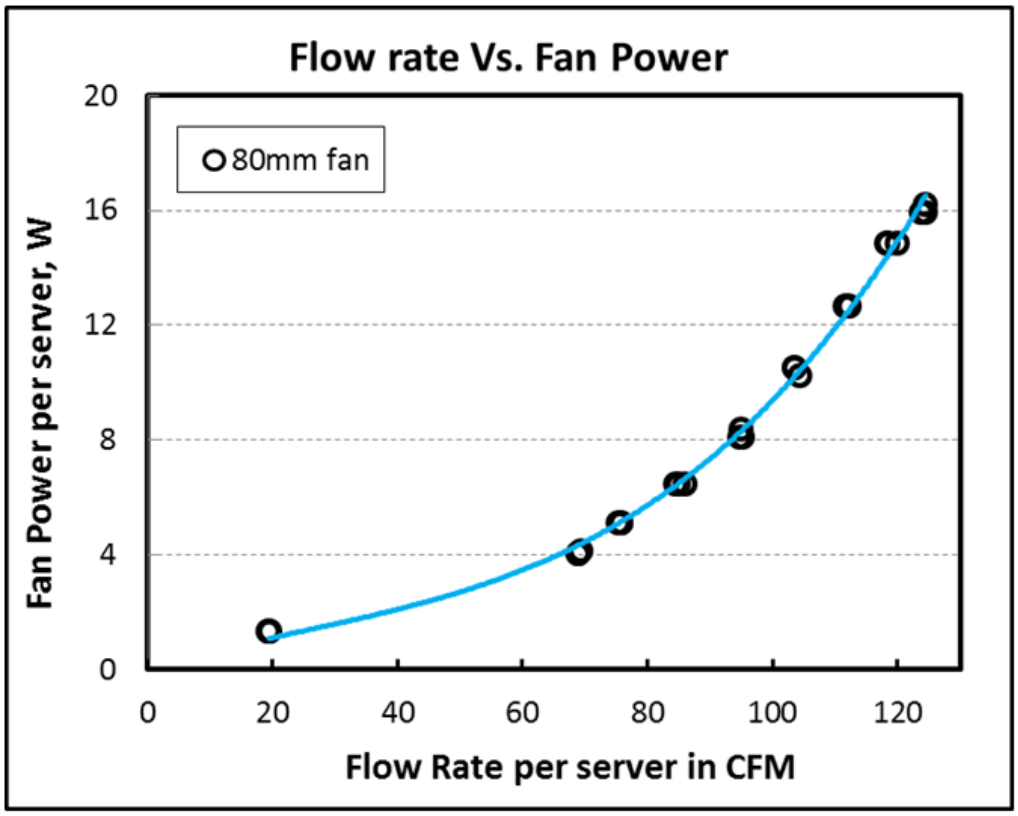

Figure 4.11: Plot representing Flow Rate vs. Fan Power for 80mm fans

4.5 Comparison of Larger Fans and Smaller Fans

4.5.1 Comparison of Flow Rate and Fan Power per Server

The following plot compares the fan power consumption vs. flow rate for the base line 60mm fan and selected 80mm fan for a single server. Clearly, 80mm fans consume less power than 60mm fans for any given flow rate. Also, the selected 80mm fans have higher capacity at its maximum fan speed and can provide less flow rate than 60mm fans when it runs at idle condition.

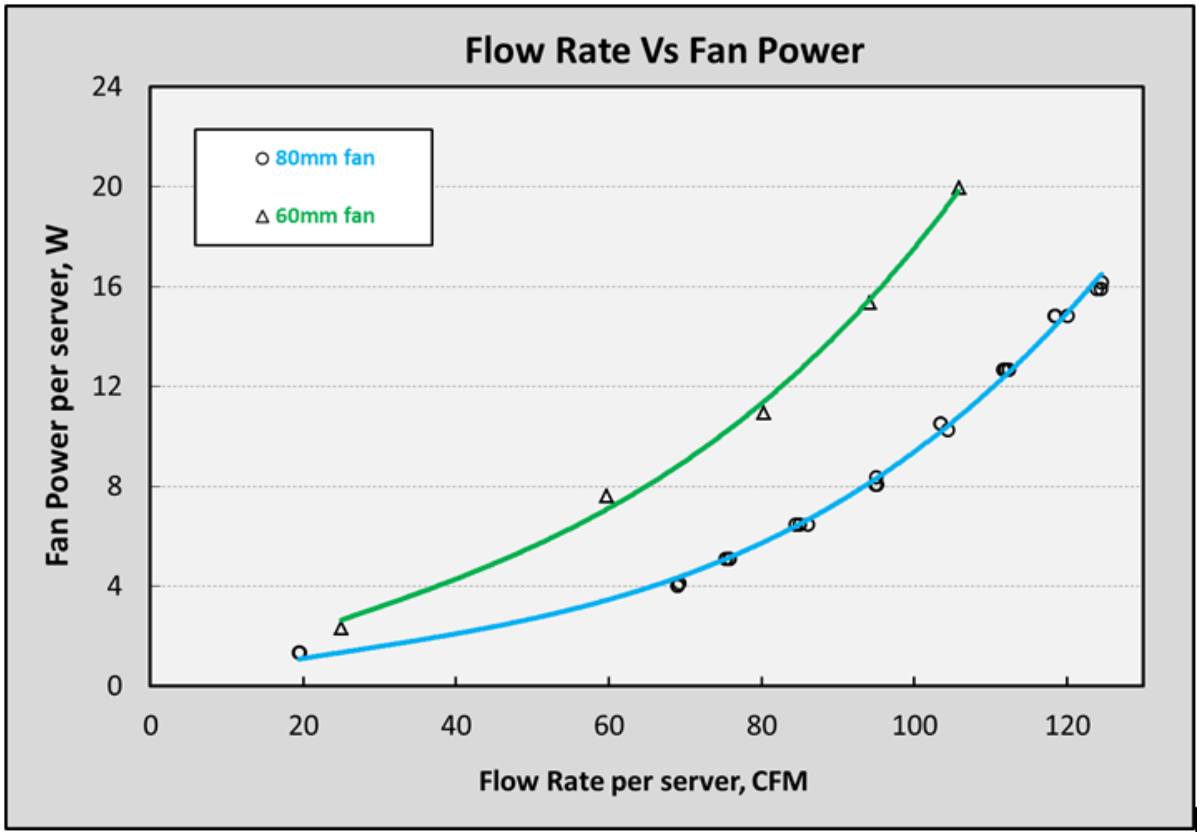

Figure 4.12: Plot for Flow Rate vs. Fan Power for 60mm and 80mm fans

4.5.2 Equation for Flow Rate and Fan Power

Sanace 9GA0812P2H0011 – 80mm fan

$y = 0.000010546541*x^3 - 0.0007862268777*x^2 + 0.067015786702455*x$

Sanace 109R0612P4J06 – 60mm fan

$y = 0.0000140610737*x^3-0.0008320912509558*x^2 + 0.1180660437953*x$

4.5.3 Calculation of saved fan power

Based on the equations and the relation between die temperature and flow rate obtained from the base line study, the fan power which is saved as result of using a larger efficient fan is estimated.

Table 4.9: Estimation of saved fan power for externally controlled fans

U_{CPU}	Flow Rate	Temperature	Fan Power			
			Sanace 80 mm	Sanace 60 mm	Difference	% saved
	CFM	°C	W	W	W	%
Idle	25	32.2	1.3	2.3	1.0	43
	60	26.4	3.4	7.6	4.2	55
	80	25.4	5.8	11.0	5.2	47
	94	25.1	8.1	15.4	7.2	47
	106	25.0	10.8	20.0	9.2	46
10%	25	41.8	1.3	2.3	1.0	43
	60	32.5	3.4	7.6	4.2	55
	80	31.6	5.8	11.0	5.2	47
	94	30.5	8.1	15.4	7.2	47
	106	30.2	10.8	20.0	9.2	46
30%	25	64.6	1.3	2.3	1.0	43
	60	44.9	3.4	7.6	4.2	55
	80	43.7	5.8	11.0	5.2	47
	94	43.0	8.1	15.4	7.2	47
	106	41.9	10.8	20.0	9.2	46
50%	25	78.3	1.3	2.3	1.0	43
	60	54.4	3.4	7.6	4.2	55
	80	52.5	5.8	11.0	5.2	47
	94	51.0	8.1	15.4	7.2	47
	106	50.0	10.8	20.0	9.2	46
70%	25	82.1	1.3	2.3	1.0	43
	60	55.6	3.4	7.6	4.2	55
	80	53.9	5.8	11.0	5.2	47
	94	52.3	8.1	15.4	7.2	47
	106	51.3	10.8	20.0	9.2	46
98%	25	87.0	1.3	2.3	1.0	43
	60	57.8	3.4	7.6	4.2	55
	80	55.3	5.8	11.0	5.2	47
	94	53.8	8.1	15.4	7.2	47
	106	53.0	10.8	20.0	9.2	46

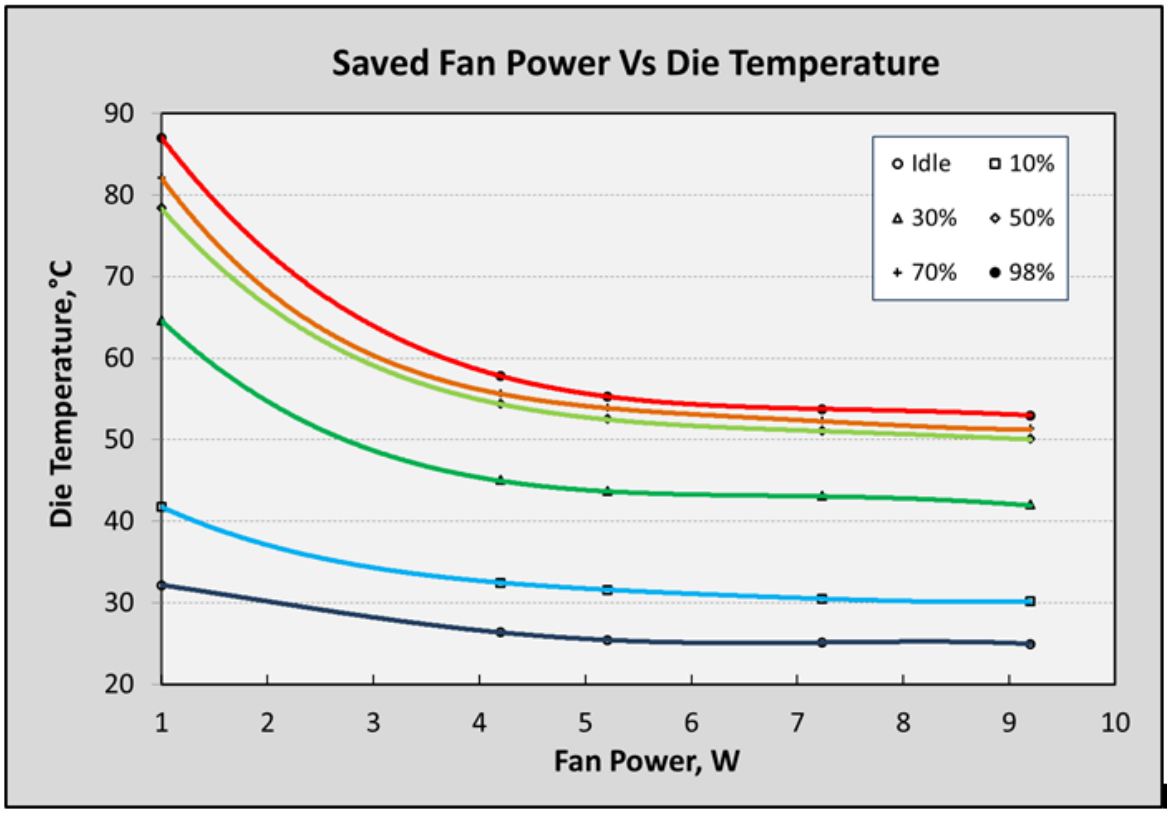

Figure 4.13: Plot to estimate saved fan power

The saved fan power depends on the utilization level and the target die temperature defined by the fan control algorithm. For the server used in the base line study, the saved fan power is estimated based on the experimental results by controlling the fans internally. The following table provides estimation of the fan power saved for the currently defined target die temperature.

Table 4.10: Estimation of saved fan power for internally controlled fans

U_{CPU}	Temperature	Fan Power			
		SanAce 80 mm	SanAce 60 mm	Difference	% saved
(%)	°C	W	W	W	%
0.1	32.7	1.4	2.4	1.0	43
10.6	39.5	1.4	2.4	1.0	43
30.6	64.6	1.4	2.4	1.0	43
50.6	71.7	1.4	2.8	1.4	49
70.5	73.6	1.5	2.9	1.4	49
98.5	73.8	1.5	3.1	1.5	50

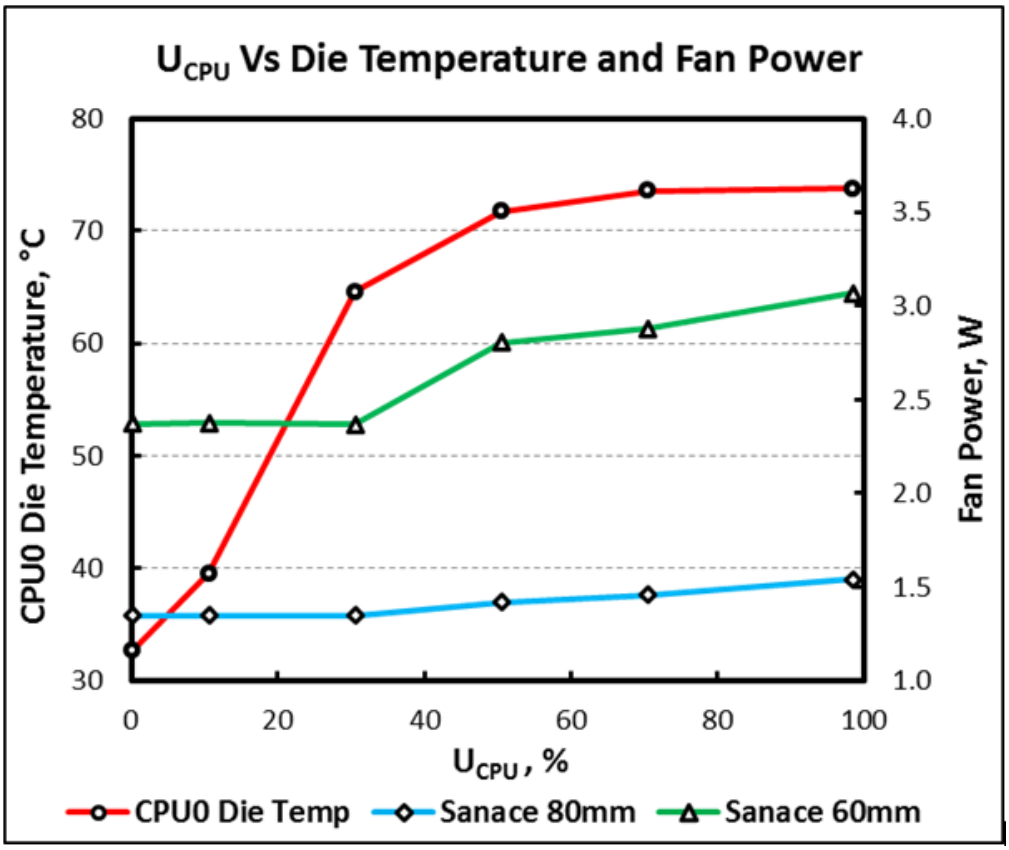

Figure 4.14: Plot to estimate saved fan power for internally controlled fans

Chapter 5

Experimental And Computational Study Of Fan Failure Scenario

5.1 Introduction

Fan failure study is performed to understand the cooling redundancy available to each server. In the base line scenario case, there are four fans catering a single server and in case of the larger fans, there are 9 fans shared by 4 servers. This study involves experimental analysis for base line server and computational simulations for larger fans.

5.2 Impact of Fan Position in a Failure Scenario on Die Temperature

The objective of this experiment is to study the effect of position of the failed fan on die temperature in fan failure scenario. In the base line case, one of the 4 fans is powered off intentionally and the die temperature is recorded and repeated for each of the 4 fans separately. To draw conclusions on the effect of fan failure, the experiment is repeated when all the fans are functioning. All fans are externally powered and externally controlled at 50% PWM duty cycle. The CPU is stressed to 98% compute utilization and the test cycle for 3 repetitions is shown in figure 5.1.

Figure 5.1: Experimental test cycle to study the position of fan failure

Following are the 5 cases considered for test and the fan numbering sequence is provided in figure 5.2

Case 1 - All fans powered on

Case 2 - Fan 4 powered off

Case 3 - Fan 3 powered off

Case 4 - Fan 2 powered off

Case 5 - Fan 1 powered off

Figure 5.2: Fan Numbering Sequence

The experiment is performed in a server installed with Centos 6.3 and the die temperature is recorded using *Sensors* Command. This command provides die temperature for each core separately and there are 6 cores in each die. Therefore the die temperature is considered as the maximum temperature of all the cores. Each test cycle takes an hour of which the last 20 minutes is considered for further analysis as this is a steady state study. The following plot shows the output for CPU0 and CPU1 die temperature as a sample for Case 1.

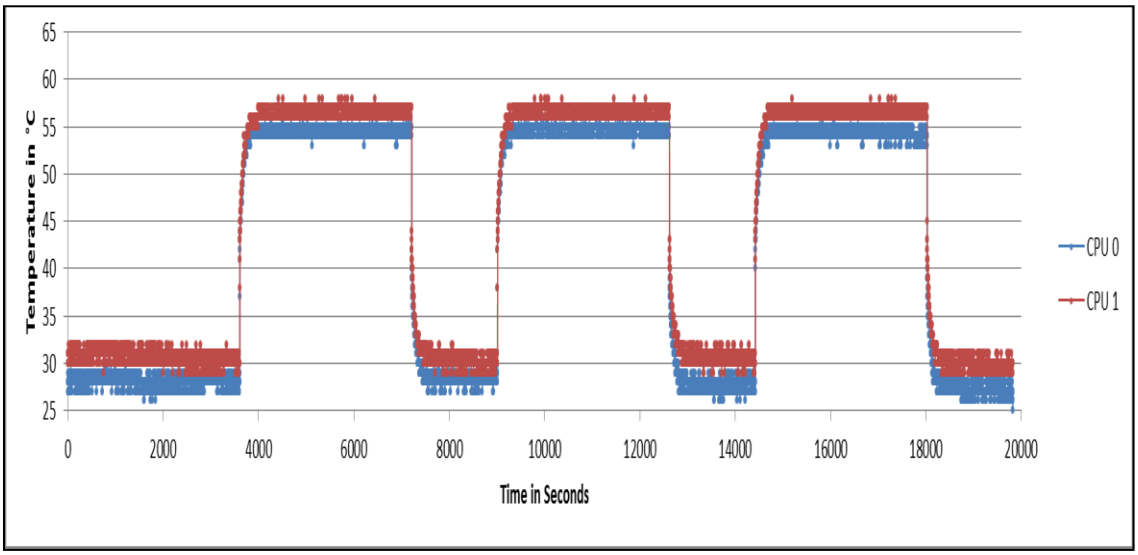

Figure 5.3: Experimental data output when all fans are powered on

From the experimental results tabulated below, it is clear that the position of the fan failure does not affect the CPU die temperature. Powering off one of four fans, increase the die temperature of CPU0 by 6.9% and CPU1 by 9.5%. Also, it is important to note that irrespective of the position of the fan failure, CPU1 die temperature is consistently higher than that of CPU0, which is due to thermal shadowing effect.

Table 5.1: Experimental results for study of impact of fan position during fan failure

		CPU 0		CPU 1	
All fans powered on	Run 1	54.7	**54.5**	56.5	**56.5**
	Run 2	54.7		56.4	
	Run 3	54.1		56.6	
Fan 1 powered off	Run 1	58.2	**58.3**	61.9	**61.9**
	Run 2	58.3		62.0	
	Run 3	58.3		61.7	
Fan 2 powered off	Run 1	58.2	**58.3**	61.9	**61.9**
	Run 2	58.5		62.0	
	Run 3	58.1		61.7	
Fan 3 powered off	Run 1	58.5	**58.5**	61.6	**61.9**
	Run 2	58.4		61.9	
	Run 3	58.5		62.1	
Fan 4 powered off	Run 1	58.4	**58.4**	61.8	**61.9**
	Run 2	58.5		62.0	
	Run 3	58.4		61.9	

5.3 Effect of fan failure when controlled by an on-board control algorithm

The objective of this experiment is to study the behaviour of fan power and die temperature, in a fan failure scenario when controlled internally by an on-board control algorithm. The experiment is conducted at 24˚C and a synthetic CPU load generator, called *lookbusy,* is used. The test cycle for this experiment is same as external fan control test in the base line study and is shown in figure 3.12. The test results for this experiment are tabulated in table 5.2.

Table 5.2: Experimental results for study fan failure for internally controlled fans

Target Utilization	Amb. Temp	CPU Util.	MEM Util.	CPU0 DT	Speed Fan 1	Speed Fan 2	Speed Fan 3	Speed Fan 4	Server Power	Fan Power	Total power
%	°C	%	%	°C	RPM	RPM	RPM	RPM	W	W	W
Idle	24.0	0.1	0.8	35.9	2020	0	2004	1981	91.3	1.81	93.1
10%	24.1	10.7	5.0	47.5	2025	0	2012	1985	119.2	1.81	121.0
30%	24.0	30.6	4.9	70.9	2352	0	2346	2288	181.7	2.06	183.8
50%	24.0	50.5	4.9	72.4	2999	0	2984	2913	217.2	2.79	219.9
70%	24.0	70.5	4.9	73.8	3050	0	3162	2966	225.4	2.92	228.3
98%	24.0	98.5	4.9	73.2	3250	0	3772	3131	232.8	3.25	236.1

This study is conducted by powering off fan 2, randomly, as it was previously established that the die temperature is independent of the position of fan failure. The effect of fan failure on die temperature and fan power is plotted.

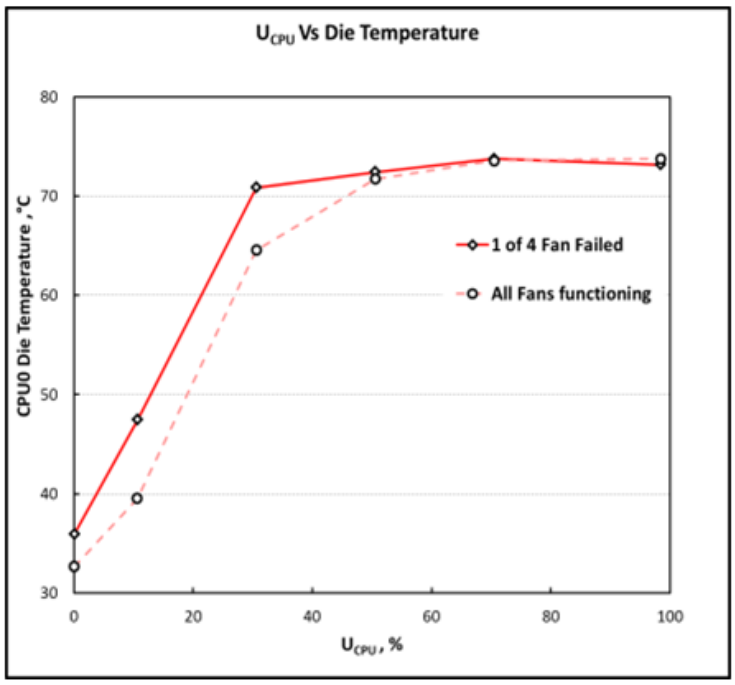

Figure 5.4: Effect of fan failure on die temperature for internally controlled fans

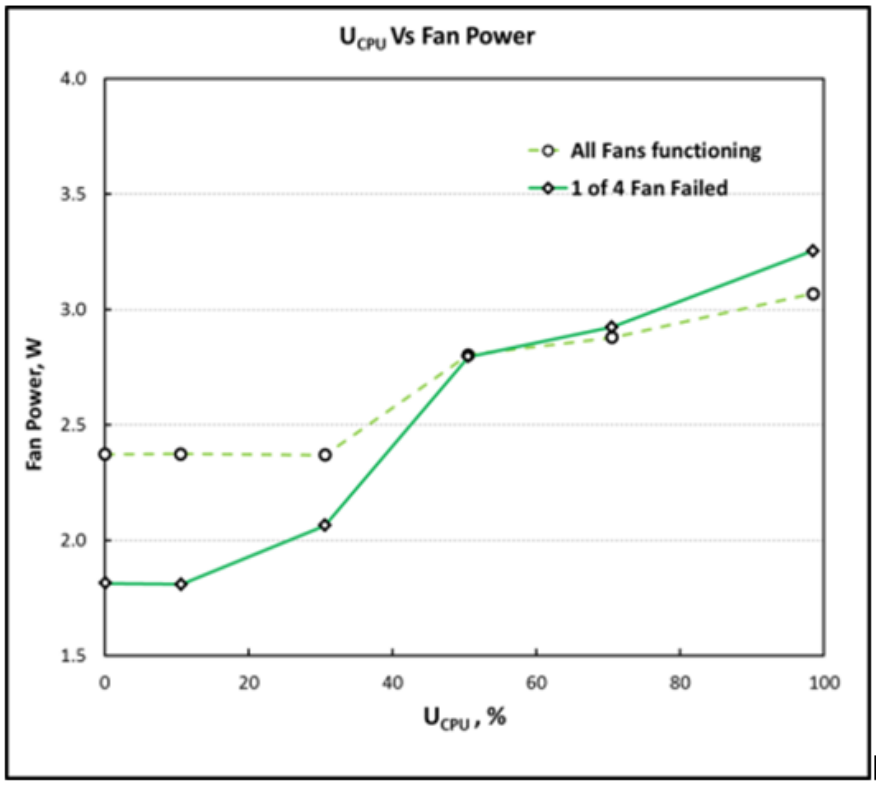

Figure 5.5: Effect of fan failure on fan power for internally controlled fans

From the plots it can be seen that the die is maintained at almost at same temperature at higher UCPU%, despite of the fan failure. Also, fan power increases to maintain the die at the predefined temperature.

5.4 Fan Failure Analysis of Larger Fans using CFD

Fan failure scenario is simulated for larger fans using CFD assuming one of the 9 fans has failed. In figure 5.6, as described in the legends, the red concentric circles with a cross inside it represent a failed fan and the green circles without the cross represent a fan that is functioning. Flow rate through each server is noted to the right of each failure scenario and the case where all the fans are functioning is at the top-right of the figure. Obviously, there is reduction in the flow rate through the server in the fan failure scenario

compared to a fully functional scenario. Comparing the flow rate across different scenario, it can be calculated that the overall flow rate through 4 servers remains almost same irrespective of the position of the failed fan.

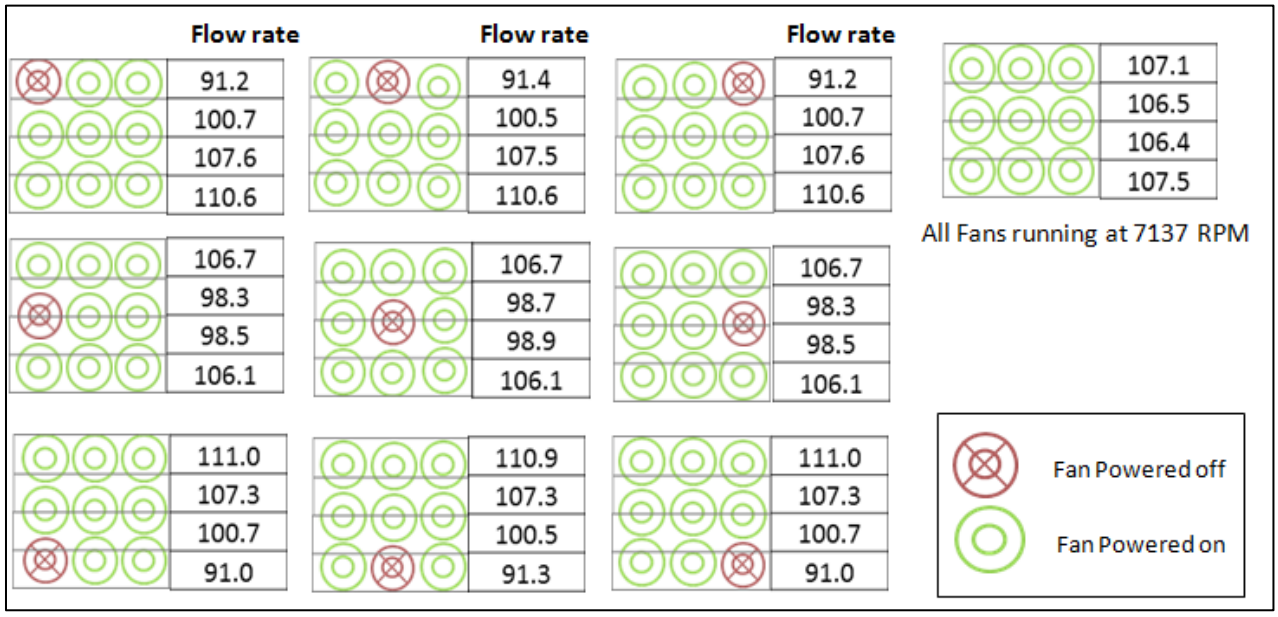

Figure 5.6: Fan failure analysis using CFD for larger fans

Chapter 6

Conclusion And Future Work

6.1 Conclusion and Discussion

Some significant overall conclusions can be drawn based on the experimental and computational analysis performed on characterizing the small fans and larger fans with the Open Compute Server.

The 80mm fans provide higher flow rate and operate at about 45% less power consumption for the corresponding flow rate. This is in concurrence with the generally accepted truth that the larger fans have better efficiency.

Increase in flow rate does reduce the die temperature but only until a threshold limit. This is due to the fact that the heat transfer is constrained by the inlet temperature and further heat transfer reduces, just as in the case of a parallel flow heat exchanger.

The actual power saving greatly depends on the fan control algorithm which defines a target die temperature. In case of the Open Compute server which is considered for this study, there is a power reduction of 1.5W for every server at higher compute utilization levels for an inlet temperature of 24˚C.

Fan selection needs to be done carefully and meticulously for IT equipment as this greatly decides the cooling power of every server, in the huge server farms. Smaller fans being less efficient below a threshold limit and use of larger fans affecting the cooling redundancy; the fan selection needs to be made appropriately.

6.2 Future Work

Experimental testing of the fan array of 80mm fans can be built and the predictions on the power consumption can be validated. Figure 6.1 shows the fan wall built for this purpose and this can be mounted with the fans.

Figure 6.1: Fan wall built to mount the 80mm fan wall array

As mentioned earlier, this study assumes compute utilization to be uniform across the four stacked servers. The study can be performed varying the utilization across the servers, in order to determine the maximum allowable deviation which shall make use of larger rack mount fans beneficial compared to smaller chassis enclosed fans.

References

1. http://www.koomey.com/post/8323374335
2. http://uptimeinstitute.com/images/stories/Uptime_Institute_2012_Data_Industry_Survey.pdf
3. http://datacenter.cit.nih.gov/interface/interface240/energy_efficiency.html
4. Joshi Y, Kumar P (2012) Energy Efficient Thermal Management of Data Centers. New York: Springer
5. http://www.datacenterknowledge.com/archives/2013/07/15/ballmer-microsoft-has-1-million-servers/
6. http://www.amca.org/UserFiles/file/ASHRAE_2012_SA-1_ppt.pdf
7. R. Jorgensen and H.R. Bahonon, "Compressibility and Fan Laws", ASHRAE Paper No. 2333
8. http://www.rotron.com/techcorner/seriesparallel.aspx
9. http://www.datacenterknowledge.com/archives/2011/04/07/closer-look-facebooks-new-open-compute-servers
10. http://ark.intel.com/products/47922
11. Pandiyan V, "Development Of Detailed Computational Flow Model Of High End Server And Validation Using Experimental Methods", Masters Thesis, The University of Texas at Arlington, 2012
12. http://www.newark.com/pdfs/datasheets/Sanyo_Denki/109R0612P4J03_A.pdf
13. http://datasheet.octopart.com/A1G280-AA79-11-EBM-Papst-datasheet-15778438.pdf
14. http://www.delta.com.tw/product/cp/dcfans/download/pdf/QFR/QFR120x120x38mm.pdf
15. http://db.sanyodenki.co.jp/product_db/cooling/dcfan/group_pdf/1356506050.pdf

Biographical Information

Bharath Nagendran recieved his Bachelor's Degree in Mechanical Engineering from Anna University, Chennai, India in May 2008. He qualified his Master of Science Degree In Mechanical Engineering at the University of Texas At Arlington in December 2013.

He was associated with Bosch, India as product design engineer in automotive wiper system. He has worked in solid modeling using CATIA V5 extensively in various automotive OEM projects.

During his Masters program he has worked in thermal management of data centers. He has associated himself with various industry collabrated research projects and studied various topics like direct/indirect evapourative cooling, cooling pads, DCIM, etc. He has worked in experimental and CFD characterization of web cache servers, efficient fan selection, thermal aware power optimization technique and determination of optimim target die temperature. He has gained theoritical background knowledge of CFD and worked data center specific CFD codes like 6SigmaDC.